ISTANBUL TECHNICAL UNIVERSITY ★ INSTITUTE OF INFORMATICS

MONITORING CHANGES OF BORDER AND AREAL EXTENT IN SALT LAKE BY USING MULTI-TEMPRORAL NOAA-AVHRR AND SPOT XS/XI IMAGES

M.Sc. Thesis by

Yelda TURKAN

705031011

Date of submission : **8 May 2006**

Date of defence examination: **14 June 2006**

Supervisor: **Prof. Dr. Filiz Sunar ERBEK**

Members of the Examining Committee **Assist. Prof. Dr.Çiğdem GÖKSEL (İ.T.Ü.)**

Prof.Dr. Muhittin GÖKMEN (İ.T.Ü.)

JUNE 2006

İSTANBUL TEKNİK ÜNİVERSİTESİ ★ BİLİŞİM ENSTİTÜSÜ

TUZ GÖLÜ'NDEKİ SINIR VE ALAN DEĞİŞİMLERİNİN ÇOK ZAMANLI NOAA-AVHRR VE SPOT XS/XI UYDU GÖRÜNTÜLERİ İLE İZLENMESİ

YÜKSEK LİSANS TEZİ

Yelda TÜRKAN
705031011

Tezin Enstitüye Verildiği Tarih : 8 Mayıs 2006
Tezin Savunulduğu Tarih : 14 Haziran 2006

Tez Danışmanı: **Prof. Dr. Filiz Sunar ERBEK**

Diğer Jüri Üyeleri: **Yard. Doç. Dr. Çiğdem GÖKSEL (İ.T.Ü.)**

Prof. Dr. Muhittin GÖKMEN (İ.T.Ü.)

HAZİRAN 2006

ACKNOWLEDGEMENTS

Firstly, I would like to express my sincere thanks to my thesis supervisor Prof. Dr. Filiz Sunar Erbek for encouraging me completing this thesis study and for sharing her wise knowledge and experience.

I would like to thank to ITU-CSCRS for SPOT data support. I would also like to thank my dear friends Ayda Akkartal, Barış Göral, Damla Uça Avcı, Göker Burak Çetin, Serkan Seröksüz who have been working in ITU-CSCRS, for their friendship and support during this study.

Final words are for my family who were very supportive and did whatever they could do to make me comfortable.

May 2006 Yelda TÜRKAN

INDEX

ABBREVIATIONS

DEM	**:** Digital Elevation Model
UV	**:** Ultraviolet
IR	**:** Infrared
EM	**:** Electromagnetic
NASA	**:** National Aeronautics and Space Administration
NOAA	**:** The National Oceanic and Atmospheric Administration
AVHRR	**:** Advanced Very High Resolution Radiometer
MODIS	**:** Moderate Resolution Imaging Spectradiometer
MERIS	**:** Medium Resolution Imaging Spectrometer
ESA	**:** European Space Agency
TM	**:** Thematic Mapper
ETM	**:** Enhanced Thematic Mapper
SPOT	**:** Systeme Pour l'Observation de la Terre
CNES	**:** French Centre National d'Etudes Spatiales
HRV	**:** Visible High-Resolution
HRVIR	**:** Visible & Infrared High-Resolution
HRG	**:** High Resolution Geometric
HRS	**:** High Resolution Stereopair
DN	**:** Digital Number
GCP	**:** Ground Control Point
RMS	**:** Root Mean Square
RGB	**:** Red-Green-Blue
SPA	**:** Specially Protected Area
WWF	**:** World Wildlife Fund
IBA	**:** Important Bird Area
UTM	**:** Universal Transversal Mercator
ISODATA	**:** Iterative Self-Organizing Data

LIST OF TABLES

Page Number:

LIST OF FIGURES

LIST OF SYMBOLS

E	: Electrical Field
M	: Magnetic Field
c	: Speed of light
λ	: Wavelength
ν	: Frequency
h	: Planck’s Constant
E	: Energy of photon
µ	: Total radiant existence from the surface of a material, Watts (W) m^{-2}
σ	: Stefan-Boltzman constant 5, $6697.10^{-8} Wm^{-2}K^{-4}$
T	: Absolute temperature (K) of the emitting material
λ	: Wavelength of maximum spectral radiant existence (µm)
A	: 2898µm°K
T	: Temperature, °K
CO_2	: Carbondioxide
τ	: Transmittance
α	: Absorptance
ρ	: Reflectance
µm	: Micrometer
km	: Kilometer
m	: Meter

MONITORING CHANGES OF BORDER AND AREAL EXTENT IN SALT LAKE BY USING MULTI-TEMPRORAL NOAA-AVHRR AND SPOT XS/XI IMAGES

SUMMARY

In the first chapter, thesis subject were briefly introduced and aim and scope of the thesis were explained.

In the second chapter, fundamentals of remote sensing were explained. Remote Sensing is the science and art of obtaining information about an object, area, or phenomenon through the analysis of data acquired by a device that is not in contact with the object, area, or phenomenon under investigation. Remote Sensing process consist of two basic stages. These are “Data acquisition” and “Data analysis”. Electromagnetic radiation principles and electromagnetic spectrum were also explained for a better understanding of remote sensing process. Besides of these, energy interactions with atmosphere and earth surfaces were explained in this chapter.

Satellite Systems were briefly explained in the third chapter. A satellite with remote sensors to observe the earth is called a remote-sensing satellite, or earth observation satellite. NOAA/AVHRR, MODIS, ENVISAT-MERIS, LANDSAT and SPOT Remote Sensing Satellite systems were introduced in details.

In the fourth chapter, digital image processing techniques were explained. Image processing and analysis can be defined as the "act of examining images for the purpose of identifying objects and judging their significance". Remote sensing images are recorded in digital forms and then processed by the computers to produce images for interpretation purposes. In a most generalized way, a digital image is an array of numbers depicting spatial distribution of a certain field parameters. Properties of a digital image were explained in this chapter. Preprocessing of a digital image were also explained. Preprocessing is an important and diverse set of image preparation programs that act to offset problems with the band data and recalculate DN values that minimize these problems. Image restoration, image

enhancement and image classification were explained in this chapter as preprocessing methods.

In the fifth chapter, study area was introduced and image processing, image enhancement, water body calculation techniques, which have been used, were explained. Salt Lake being the second largest lake in Turkey is a very important source of salt for Turkey. Since covering very large area in winter and not freezing even coldest days, it is an important area for aquatic birds to spend their winter time. Salt Lake is also declared as an “A class water area” according to International criteria. Hence, the changes in areal extent of Salt Lake is important both for aquatic birds habitat and also the ecosystem of the lake. In this study, NOAA-AVHRR (dated between 1997-2004) and SPOT XS/XI (dated 2005) images were processed to evaluate the temporal and annual changes in the lake.

Finally, results were evaluated and discussed in the sixth chapter. Generally, water body areal extents calculated with digitizing technique greater than segmentation and ISODATA techniques. It was found that areal extents are being changed regarding to temproral and annual base. Meteorological data of Konya were also used for interpreting the results obtained. Hence, meteorological data and areal extent results were seen that they were compatible.

TUZ GÖLÜ'NDEKİ SINIR VE ALAN DEĞİŞİMLERİNİN ÇOK ZAMANLI NOAA-AVHRR VE SPOT XS/XI UYDU GÖRÜNTÜLERİ İLE İZLENMESİ

ÖZET

Tez konusu ve tezin amacı ile kapsamı birinci bölümde ele alınmıştır.

İkinci bölümde, Uzaktan Algılama biliminin temel noktaları açıklanmıştır. Uzaktan Algılama, bir algılayıcı ile algılanmış veriden bir nesne, alan veya olay hakkında, arada herhangi bir fiziksel temas olmaksızın, bilgi çıkartan, yorumlayan bir bilim ve sanat dalıdır. Uzaktan Algılama süreci iki temel aşamadan meydana gelir. Bunlar "veri elde etme" ve "veri analizi" aşamalarıdır. Elektromanyetik ışınım prensipleri ve elektromanyetik spektrum özellikleri uzaktan algılama sürecinin daha iyi anlaşılması için kısaca açıklanmıştır. Ayrıca, atmosfer ve yer yüzeyleri ile enerji etkileşimleri de bu bölümde açıklanmıştır.

Uydu sistemleri üçüncü bölümde anlatılmıştır. Uzaktan Algılama amaçlı algılayıcıları bulunan uydulara "Uzaktan Algılama uyduları" veya "Dünya Gözlem uyduları" adı verilir. NOAA/AVHRR, MODIS, ENVISAT-MERIS, LANDSAT ve SPOT uzaktan algılama sistemleri daha detaylı biçimde verilmiştir.

Dördüncü bölümde, Sayısal görüntü işleme teknikleri anlatılmıştır. Görüntü işleme ve analizi "objeleri teşhis etme ve önemlerine karar verme amacı ile görüntülerin dikkatle gözden geçirilmesi" olarak tanımlanabilir. Uzaktan algılama görüntüleri sayısal biçimde kayıt edilir ve yorumlamak için bilgisayarlar aracılığı ile görüntü formatına dönüştürülür. En genel anlatım ile, sayısal görüntü, kesin alan parametrelerinin sayı dizilerinin uzaysal dağılımı ile ilişkilendirilerek anlatılmasıdır. Sayısal görüntünün özellikleri ve önişleme aşaması da bu bölümde anlatılmıştır. Önişleme, band verisinde var olan ofset problemlerine yönelik olarak çalışan ve piksel değerlerini yeniden hesaplayarak bu problemleri en aza indirgeyen, önemli ve geniş kapsamlı görüntü hazırlama programıdır. Görüntü restorasyonu, görüntü iyileştirmesi ve görüntü sınıflandırma yöntemleri bu bölümde önişleme yöntemleri olarak ele alınmıştır.

Beşinci bölümde, çalışma bölgesi hakkında bilgi verilmiş ve kullanılan görüntü işleme, görüntü iyileştirme, su alanı hesaplama yöntemleri açıklanmıştır. Tuz Gölü, Türkiye'nin ikinci büyük gölü olup, Türkiye için önemli bir Tuz kaynağıdır. Tuz Gölü kış aylarında kapladığı büyük su alanı ve en soğuk günlerde bile donmaması sebebi ile, sucul kuşların kış aylarını geçirmeleri için önemli bir sulak alandır. Tuz Gölü, uluslarası kriterlere göre A sınıfı su alanı ilan edilmiştir. Dolayısı ile, Tuz Gölünün su alanındaki değişim sucul kuşlar ve gölün ekosistemi için önemlidir. . Bu çalışmada, NOAA-AVHRR (1997-2004 tarihleri arasında) ve SPOT XS/XI görüntüleri (2005 tarihli), gölde mevsim ve yıllara göre meydana gelen alansal değişimi değerlendirmek amacı ile işlenmiştir.

Son bölümde, sonuçlar değerlendirilip, tartışıldı. Genel olarak, sayısallaştırma yöntemi ile hesaplanan su alanının, segmentasyon ve ISODATA sınıflandırma yöntemi ile hesaplanandan daha fazla olduğu gözlendi. Göldeki su alanı miktarı mevsim ve yıllara bağlı olarak değişmektedir. Konya ilinin meteorolojik verileri yorumlama amacı ile kullanılmıştır. Su alanı miktarları ve meteorolojik verilerin birbiri ile uyuştuğu gözlenmiştir.

1. INTRODUCTION

1.1. Introduction

Salt lake being the second largest lake in Turkey is a very important source of salt for Turkey. Salt Lake extent varies greatly with a maximum depth in spring of 1.5 m and most of the lake drying up in summer. The area receives the lowest annual precipitation in Turkey. The lake is fed by two major streams, groundwater and surface water. An unnaturally constant input is the waste water which reaches the lake through the 150 km-long Konya drain. Brackish marshes have formed where channels and streams enter the lake, and the lake is surrounded by (only partially irrigated) cereal fields in the north, east and west, whilst extensive seasonally-flooded salt-steppe occur, particularly to the south-west.

Since covering very large area in winter and not freezing even coldest days, it is an important area for aquatic birds to spend their winter time. Salt Lake is also declared as an “A class water area” according to International criteria. Hence, the changes in areal extent of Salt Lake is important both for aquatic birds habitat and also the ecosystem of the lake. In this study, NOAA-AVHRR (dated between 1997-2004) and SPOT XS/XI (dated 2005) images were processed to evaluate the temporal and annual changes in the lake.

1.2. Aim and Scope

Salt Lake was declared as a Specially Protected Area (SPA) in 1992. Because, Salt Lake holds the main Turkish breeding colony of Greater Flamingo which breed on a group of islands in the southern part of the lake. Lesser Kestrel, Avocet and Greater Sand plover also breed. Consequently, Salt Lake is an Important Bird Area (IBA).

The main channel (completed in 1974) which drains the entire Konya irrigation area (IBA no. 67, 68 and 69) is 150 km-long and runs north from the irrigation area by-passing two other IBAs (Bolluk Lake [IBA no. 70] and Tersakan Lake [IBA no. 71]) before flowing into Salt Lake just 10 km from the flamingo breeding islands.

The changes in areal extent of Salt Lake is important both for aquatic birds habitat and also the ecosystem of the lake as mentioned above. In this study, NOAA-AVHRR and SPOT XS/XI images were processed to calculate water body areal extent of the lake. These processes did not take so much time. If these areal extent calculations were done classical methods, it will be take so much time and money. Hence, Remote Sensing is efficient and cost effective method for water body areas applications.

2. FUNDAMENTALS OF REMOTE SENSING

2.1 Remote Sensing

Remote Sensing is the science and art of obtaining information about an object, area, or phenomenon through the analysis of data acquired by a device that is not in contact with the object, area, or phenomenon under investigation. [1]

There are many application areas of Remote Sensing. Some of these are;

- Agriculture (crop type mapping, crop monitoring and damage assessment),
- Forestry (clear cut mapping and deforestation, species identification and typing, burn mapping),
- Geology (structural mapping and terrain analysis),
- Hydrology (flood delineation and mapping, soil moisture),
- Sea ice (ice type and concentration, ice motion),
- Land cover (land use change, land cover and biomass mapping),
- Mapping (planimetry, DEMs, topographic and baseline thematic mapping),
- Oceans and coastal monitoring (ocean features, ocean colour & phytoplankton concentration, oil spill detection) (Figure 2.1).

Figure 2.1 Application areas of Remote Sensing [2]

There are two types of Remote Sensing processes in respect to the type of energy resources. These are *Passive Remote Sensing* and *Active Remote Sensing*.

Passive Remote Sensing: Makes use of sensors that detect the reflected or emitted electro-magnetic radiation from natural sources.

Active Remote Sensing: Makes use of sensors that detect reflected responses from objects that are irradiated from artificially-generated energy sources, such as radar. [3]

Remote Sensing process consist of two basic stages. These are "Data acquisition" and "Data analysis" (Figure 2.2).

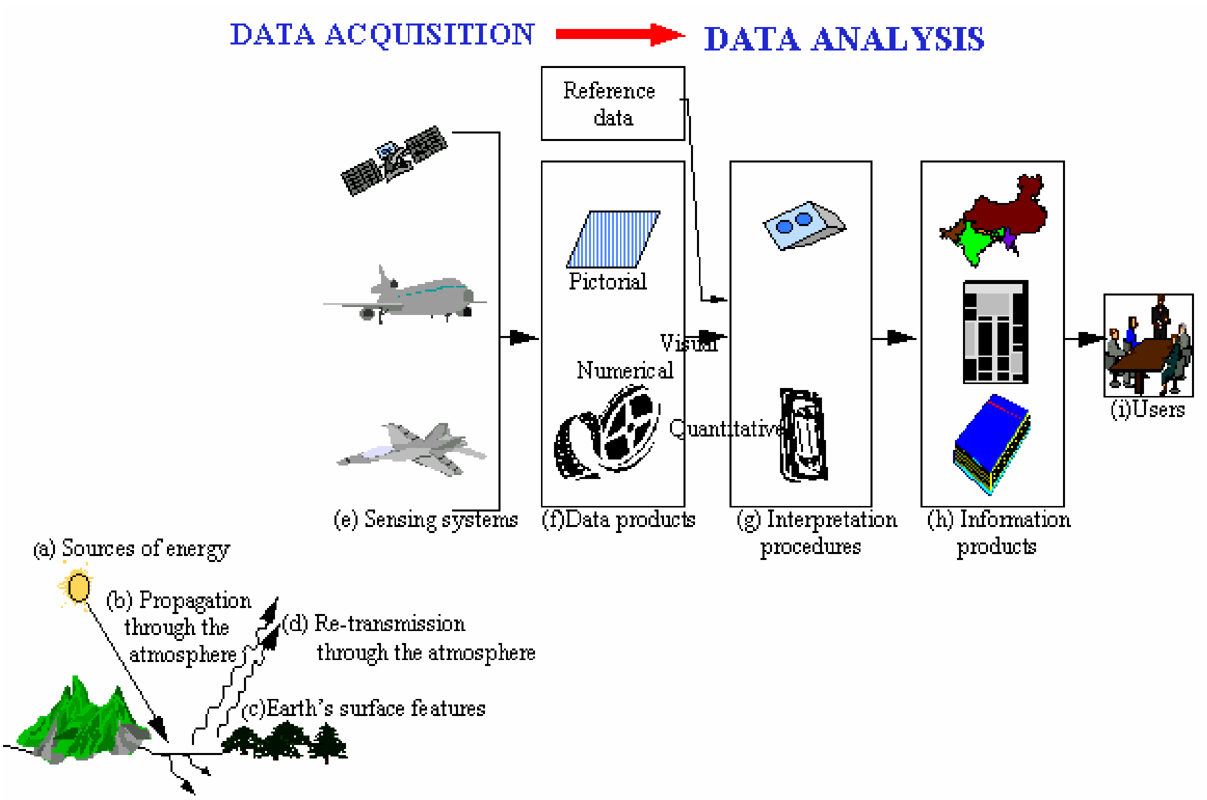

Figure 2.2 Remote Sensing process [17]

2.1.1 Data Acquisition

Energy Source or Illumination - the first requirement for remote sensing is to have an energy source, which illuminates or provides electromagnetic energy to the target of interest.

Radiation and the Atmosphere - as the energy travels from its source to the target, it will come in contact with and interact with the atmosphere it passes through. This interaction may take place a second time as the energy travels from the target to the sensor.

Interaction with the Target - once the energy makes its way to the target through the atmosphere, it interacts with the target depending on the properties of both the target and the radiation.

Recording of Energy by the Sensor - after the energy has been scattered by, or emitted from the target, we require a sensor (remote - not in contact with the target) to collect and record the electromagnetic radiation.

Transmission, Reception, and Processing - the energy recorded by the sensor has to be transmitted, often in electronic form, to a receiving and processing station where the data are processed into an image (hardcopy and/or digital). [2]

2.1.2 Data Analysis

Interpretation and Analysis - the processed image is interpreted, visually and/or digitally or electronically, to extract information about the target, which was illuminated.

Application - the final element of the remote sensing process is achieved when the information is applied to extract from the imagery about the target in order to better understand it, reveal some new information, or assist in solving a particular problem. [2]

2.2 Electromagnetic Energy

2.2.1 Electromagnetic Radiation Principles

Electromagnetic energy is emitted and reflected by the various earth surface features on the way sensor acquire data. [1] All electromagnetic radiation has fundamental properties and behaves in predictable ways according to the basics of wave theory. Electromagnetic radiation consists of an electrical field (E), which varies, in magnitude in a direction perpendicular to the direction in which the radiation is traveling, and a magnetic field (M) oriented at right angles to the electrical field (Figure 2.3). Both these fields travel at the speed of light (c). [2]

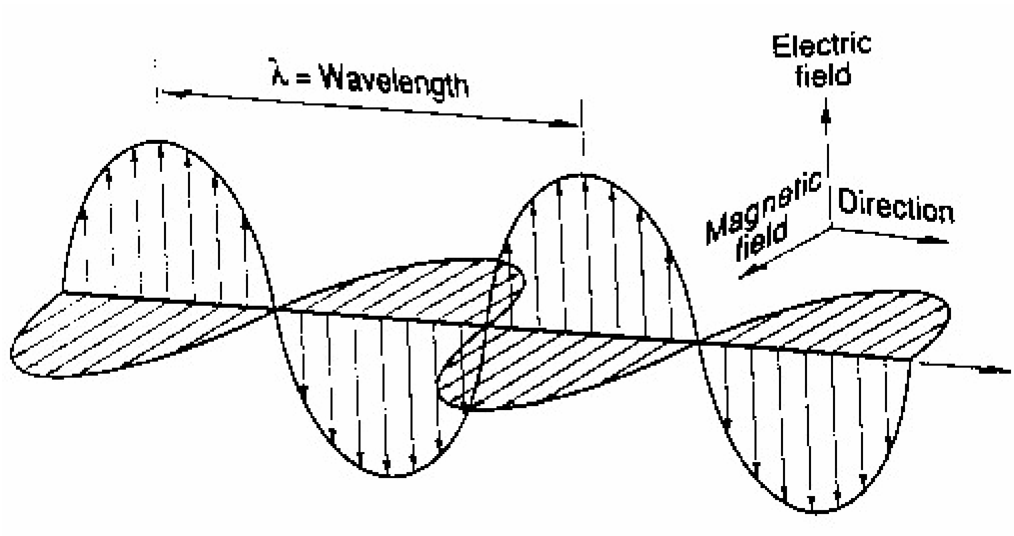

Figure 2.3 Propagation of electromagnetic wave [21]

Two characteristics of electromagnetic radiation are particularly important for understanding remote sensing. These are the *wavelength and frequency* (Figure 2.4).

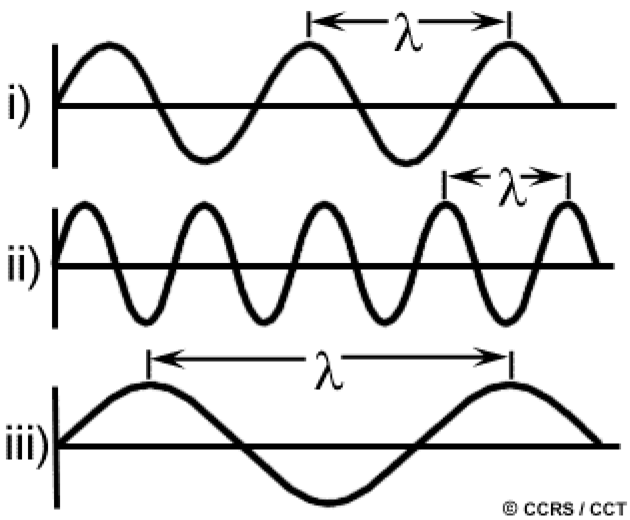

Figure 2.4 Wavelengths in different length [2]

Wavelength and frequency are related by the following formula:

$$c=\lambda\nu \tag{2.1}$$

where

λ = wavelength(m)

ν = frequency(Hz)

c = Speed of light ($3 * 10^8$ m/saniye)

Therefore, the two are inversely related to each other. The shorter the wavelength, the higher the frequency. Understanding the characteristics of electromagnetic radiation in terms of their wavelength and frequency is crucial to understanding the information to be extracted from remote sensing data. [2]

However many characteristics of electromagnetic radiation can be explained by wave theory, it can be useful to investigate the quantum nature of electromagnetic radiation. According to quantum nature the energy of a quantum is directly proportional to the frequency of the radiation. The amount of this energy is determined by using Planck's general equation:

$$E=h\nu \tag{2.2}$$

where:

h = Planck's constant (6.6260…x 10^{-34} Joules-sec)

ν = frequency

E = energy of photon

The equation is the proof of photons traveling at higher frequencies are more energetic. [4] Therefore the longer waves have less energy while there is an inverse proportion between wavelength and frequency.

Sun is known as to be the source radiator for remote sensing on the other hand all objects at temperatures above absolute zero emits radiation. Moreover the amount of energy any object radiates is, among other things, a function of the surface temperature of the object. This property is expressed by the Stefan-Boltzman law.

$$\mu=\sigma.T^4 \tag{2.3}$$

where:

μ = total radiant existence from the surface of a material, Watts (W) m^{-2}

σ = Stefan-Boltzman constant 5, $6697.10^{-8}Wm^{-2}K^{-4}$

T = absolute temperature (K) of the emitting material

This relation, given in the formula, can be applied to all wavelengths of the spectrum shorter than the microwave region, however, the radiation changes to μ=f (T), that is the power varies directly and linearly as the temperature in degrees Kelvin. [5]

In addition Planck curve is defined by Planck's general equation either for each absolute temperature (°K). The magnitude of this area that lay under the curve is equal to the total electromagnetic energy emitted. Stephan-Boltzman Law equation also gives this area under Planck curve. Blackbody is a hypothetical substance that conforms to this curve [2] and is an ideal radiator that totally absorbs and reemits all energy incident upon it. [1] The sun is close to blackbody, but many terrestrial objects are quite different (Figure 2.5).

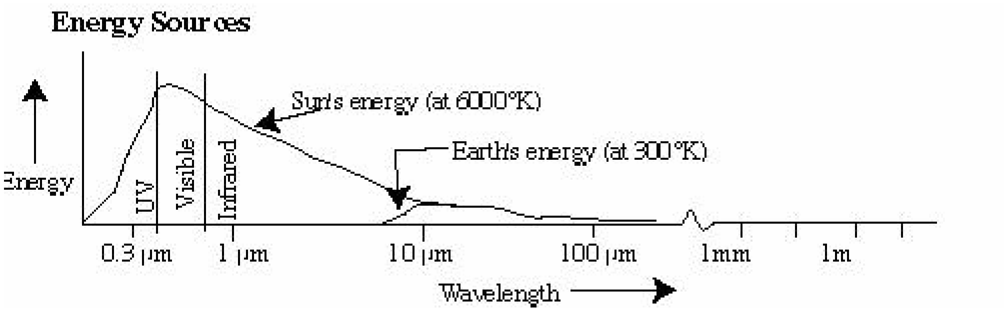

Figure 2.5 Blackbody curve at 6000°K and 300°K [18]

The wavelength near which most of the radiation is emitted depends on the temperature of the object. This fact is represented by Wien's displacement law.

$$\Lambda_m = A/T \tag{2.4}$$

λ = wavelength of maximum spectral radiant existence (μm)

A = 2898μm°K

T = temperature, °K

λ gives the dominant wavelength at which a blackbody curve reaches a maximum also it is inversely proportional to absolute temperature.

2.2.2 Electromagnetic Spectrum

Electromagnetic radiation extends over a wide range of energies and wavelengths (frequencies). The distribution of the continuum of all radiant energies can be plotted either as a function of wavelength or of frequency in a chart known as the electromagnetic spectrum and it ranges from the shorter wavelengths (including gamma and x-rays) to the longer wavelengths (including microwaves and broadcast radio waves). Using spectroscopes and other radiation detection instruments, over the years scientists have arbitrarily divided the electromagnetic spectrum into regions or intervals and applied descriptive names to them (Figure 2.6). [4]

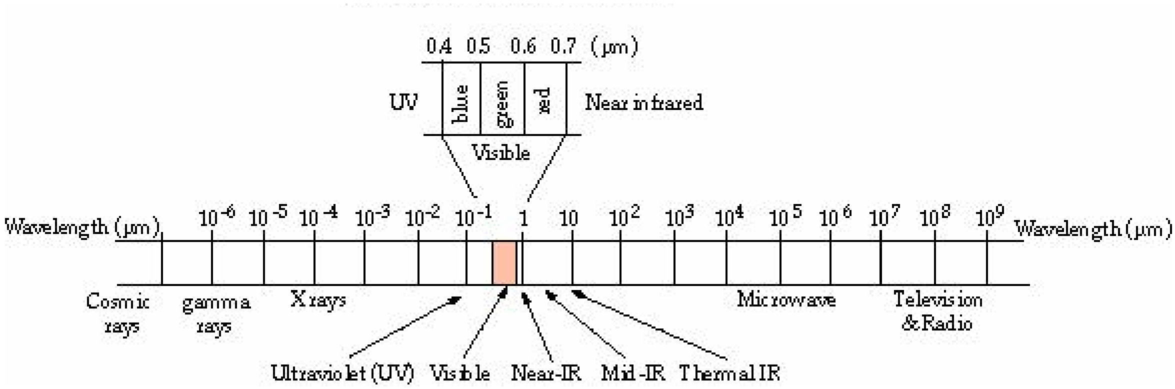

Figure 2.6 Electromagnetic spectrum [18]

The ultraviolet or UV portion of the spectrum has the shortest wavelengths, which are practical for remote sensing. Some Earth surface materials, primarily rocks and minerals, fluoresce or emit visible light when illuminated by UV radiation.

The light which human eyes can detect is part of the visible spectrum. The visible wavelengths cover a range from approximately 0.4 to 0.7 μm. The longest visible wavelength is red and the shortest is violet. It is important to note that this is the only portion of the spectrum that can be associated with the concept of colors.

- Blue: 0.446 - 0.500 μm
- Green: 0.500 - 0.578 μm
- Red: 0.620 - 0.7 μm

The infrared (IR) region which covers the wavelength range from approximately 0.7 μm to 100 μm. The infrared region can be divided into two categories based on their radiation properties – the near IR, and the thermal IR. Radiation in the near IR region is used for remote sensing purposes in ways very similar to radiation in the visible portion. The near IR covers wavelengths from approximately 0.7 μm to 3.0 μm. The thermal IR region is quite different than the visible and near IR portions, as this energy is essentially the radiation that is emitted from the Earth's surface in the form of heat. The thermal IR covers wavelengths from approximately 3.0 μm to 100 μm.

The portion of the spectrum of more recent interest to remote sensing is the microwave region from about 1 mm to 1 m. This covers the longest wavelengths used for remote sensing. The shorter wavelengths have properties similar to the thermal infrared region while the longer wavelengths approach the wavelengths used for radio broadcasts. [2]

2.3 Energy Interactions with Atmosphere and Earth Surface

2.3.1 Atmospheric Attenuation

As electromagnetic radiation propagates through the atmosphere, it will interact with the various species it encounters. This interaction may, take form of scattering, where energy is not lost but merely redirected or of absorption, where energy is absorbed (and to conserve energy, ultimately reradiated although again in different range of wavelengths). In either case, energy is lost from the forward direction and the combined affect of scattering is called attenuation. [7]

2.3.1.1 Scattering

Scattering is the redirection of electromagnetic radiation by particles suspended in the atmosphere or by large molecules of atmospheric gases. How much scattering takes place depends on several factors including the wavelength of the radiation, the abundance of particles or gases, and the distance the radiation travels through the atmosphere. [2]

Theoretically scattering can be divided into three categories depending upon the wavelength of radiation being scattered and the size of the particles causing the scattering. These three categories are Rayleigh, Mie and non-selective scattering. [8]

2.3.1.2 Absorption

In contrast to scattering, this phenomenon causes molecules in the atmosphere to absorb energy at various wavelengths. Ozone, carbon dioxide, and water vapor are the three main atmospheric constituents which absorb radiation.

Ozone serves to absorb the harmful (to most living things) ultraviolet radiation from the sun. This is because CO_2 tends to absorb radiation strongly in the far infrared portion of the spectrum - that area associated with thermal heating - which serves to trap this heat inside the atmosphere. Water vapor in the atmosphere absorbs much of the incoming longwave infrared and shortwave microwave radiation. [2]

2.3.1.3 Atmospheric Windows

Some types of electromagnetic radiation easily pass through the atmosphere, while other types do not. The ability of the atmosphere to allow radiation to pass through it is referred to as its transmissivity, and varies with the wavelength/type of the radiation. The gases that comprise our atmosphere absorb radiation in certain wavelengths while allowing radiation with differing wavelengths to pass through.

The areas of the EM spectrum that are absorbed by atmospheric gases such as water vapor, carbon dioxide, and ozone are known as absorption bands. In the Figure 2.7, absorption bands are represented by a low transmission value that is associated with a specific range of wavelengths.

In contrast to the absorption bands, there are areas of the electromagnetic spectrum where the atmosphere is transparent (little or no absorption of radiation) to specific wavelengths. These wavelength bands are known as atmospheric "windows" since they allow the radiation to easily pass through the atmosphere to Earth's surface.

Most remote sensing instruments on aircraft or space-based platforms operate in one or more of these windows by making their measurements with detectors tuned to specific frequencies (wavelengths) that pass through the atmosphere. Remote sensing instrument collects and records the radiant energy that is reflected sunlight or emitted heat from an object. While most remote sensing systems are designed to collect reflected radiation, some sensors, especially those on meteorological satellites, directly measure absorption phenomena, such as those associated with carbon dioxide (CO2) and other gases. The atmosphere is nearly opaque to EM radiation in part of the mid-IR and all of the far-IR regions. In the microwave region, by contrast, most of this radiation moves through unimpeded, so radar waves reach the surface (although weather radars are able to detect clouds and precipitation because they are tuned to observe backscattered radiation from liquid and ice particles). [9]

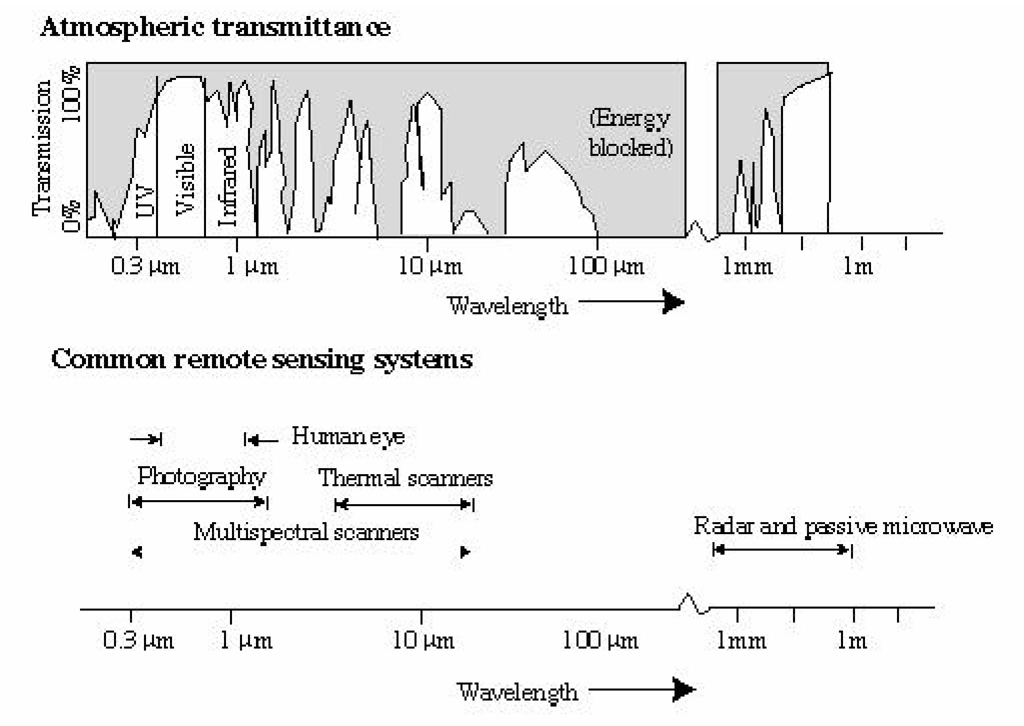

Figure 2.7 Atmospheric windows [18]

2.3.2 Interactions with Earth Surface Features

Radiation that is not absorbed or scattered in the atmosphere can reach and interact with the Earth's surface. There are three (3) forms of interaction that can take place when energy strikes, or is incident (I) upon the surface (Figure 2.8). [2]

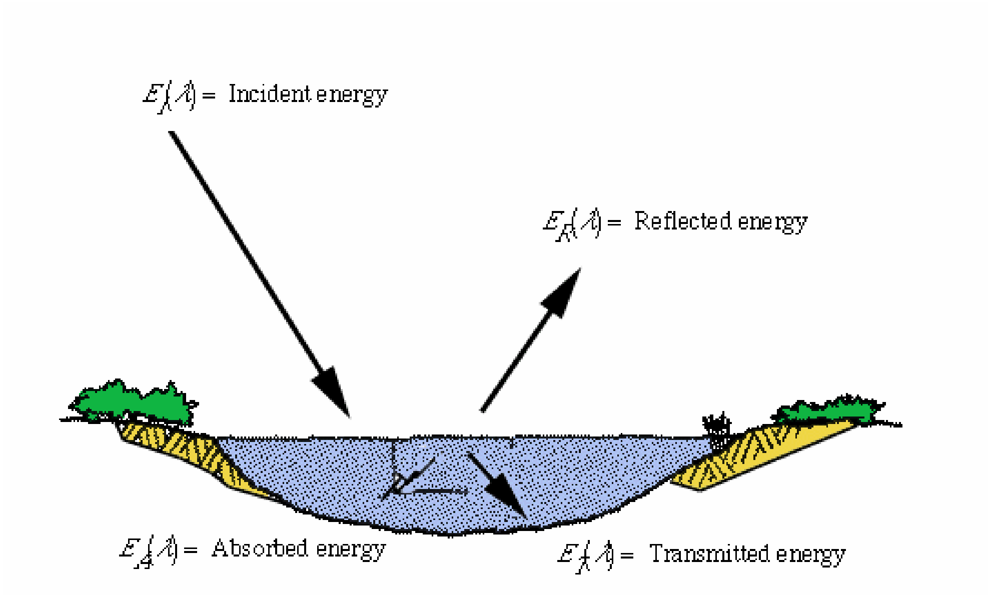

Figure 2.8 Interactions with earth surface features [19]

* Transmittance (τ) – some of the incident radiation penetrates into certain surface materials such as water and if the material is transparent and thin in one dimension, normally passes through, generally with some diminution.

* Absorptance (α) – some of the incident radiation is absorbed through electron or molecular reactions within the medium; a portion of this energy is then re-emitted, usually at longer wavelengths, and some of it remains and heats the target.

* Reflectance (ρ) - some of the incident radiation (commonly 100%) reflects (moves away from the target) and scatters away from the target at various angles, depending on the surface roughness and the angle of incidence of the rays. [4]

These three forms expressed as ratios (commonly as percentages) to the incident radiation. The ratios differ as a function of chemical-physical characteristics of the matter that the incident radiation encounters. Due to the law of conservation of energy:

$$\tau + \alpha + \rho = 1 \tag{2.5}$$

The way the incident radiation interacts with the surface is strictly dependent on the incident energy wavelength. This implies that the same surface features can be distinguished in a given spectral interval, and cannot be identified in another spectral range.

The reflection of the incident radiation is also strictly related to the surface geometric characteristics. There are two general types of reflecting surfaces that interact with EMR: specular (smooth) and diffuse (rough) (Figure 2.9). These terms are defined geometrically, not physically. The Rayleigh criterion is used to determine surface roughness with respect to radiation:

$$\lambda/8\cos\theta \tag{2.6}$$

where h is the surface irregularity height (measured in Angstroms), λ is the wavelength (also in Angstroms) and θ is the angle of incidence (measured from the normal (perpendicular) to the surface. If λ is less than h, the surface acts as a diffuse reflector; if greater than h, the surface is specular. [4]

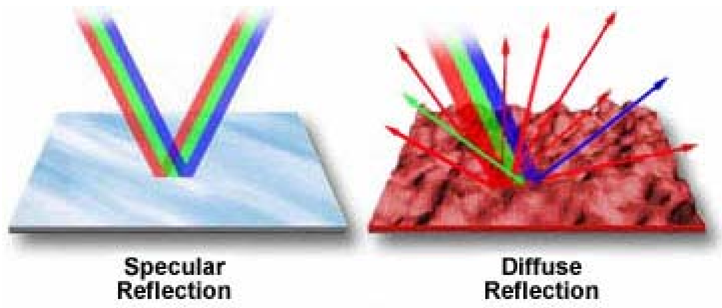

Figure 2.9 Specular and Diffuse reflection [20]

2.3.3 Spectral Reflectance of Earth Features

Spectral reflectance is assumed to be different with respect to the type of land cover. This is the principle that in many cases allows the identification of land cover with remote sensing by observing the spectral reflectance or spectral radiance from a distance far removed from the surface. [31] A spectral reflectance curve is a graph of the spectral reflectance of an object as a function of wavelength and is very useful for choosing the wavelength regions for remotely sensed data acquisition.

Figure 2.10 shows typical spectral reflectance curves for three basic types of earth features: healthy green vegetation, dry bare soil, and clear lake water. The lines in this figure represent average reflectance curves compiled by measuring a large sample of features. In general, the configuration of these curves is an indicator of the type and condition of the features to which they apply. Although the reflectance of individual features will vary considerably above and below average, these curves demonstrate some fundamental points concerning spectral reflectance. [1]

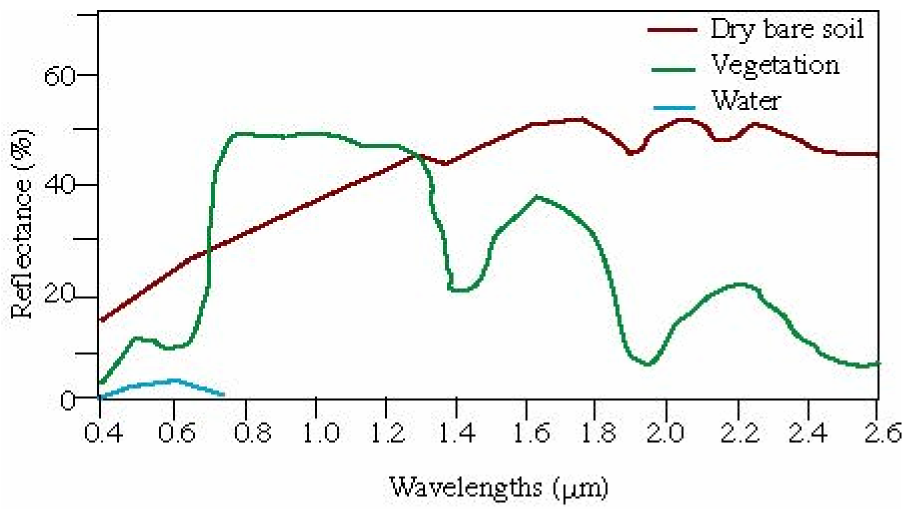

Figure 2.10 Typical spectral reflectance curves for vegetation, soil and water [18]

2.3.3.1 Spectral Reflectance of Vegetation

Spectral reflectance curves for healthy green vegetation almost always manifest the "peak and valley" configuration illustrated in Figure 2.10. The valleys in the visible portion of the spectrum are dictated by the pigments in plant leaves. Chlorophyll, for example, strongly absorbs energy in the wavelength bands centered at about 0.45 and 0.67 μm. Human eyes perceive healthy vegetation as green in color because of the very high absorption of blue and red energy by plant leaves and the very high reflection of green energy. If a plant is subject to some form stress that interrupts its normal growth and productivity, it may decrease or cease chlorophyll production. The result is less chlorophyll absorption in the blue and red bands. Often the red reflectance increases to the point that we see the plant turn yellow (combination of green and red).

The vegetation reflectance rapidly increases at wavelenghts between 0.7 and 0.75 μm. In the range from about 0.7 to 1.3μm, a plant leaf typically reflects 40 to 50 percent of the energy incident upon it. Most of the remaining energy is transmitted, since absorption in this spectral region in minimal (less than 5 percent). Plant reflectance in the range 0.7 to 1.3 μm results primarily from the internal structure of plant leaves. Because this structure is highly variable between plant species, reflectance measuruments in this range make easier discriminating between species, even if they look the same in visible wavelengths. Likewise, many plant stresses alter the reflectance in this region and sensors operating in this range are often used for vegetation stress detection. Also, multiple layers of leaves in a plant canopy provide the opportunity for multiple transmittance and reflectance. Hence, the near infrared reflectance increases with the number of layers of leaves in a canopy, with the reflection maximum achieved at about eight leaf layers.

Beyond 1.3 μm, energy incident upon vegetation is essentially absorbed or reflected, with little to no transmittance of energy. Dips in reflectance occur at 1.4, 1.9 and 2.7 μm because water in the leaf absorbs strongly at these wavelengths. Accordingly, wavelengths in these spectral regions are referred to as water absorption bands. Reflectance peaks occur at about 1.6 and 2.2 μm, between the absorption bands. Throughout the range beyond 1.3 μm, leaf reflectance is approximately inversely related to the total water present in a leaf. This total is a function of both the moisture content and the thickness of a leaf. [1]

2.3.3.2 Spectral Reflectance of Soil

The soil curve in Figure 2.10 shows considerably less peak and valley variation in reflectance. That is, the factors that influence soil reflectance act over less specific spectral bands. Some of the factors affecting soil reflectance are moisture content, soil texture (proportion of sand, silt and clay), surface roughness, presence of iron oxide, and organic matter content. These factors are complex, variable, and interrelated. For example, the presence of moisture in soil will decrease its reflectance. As with vegetation, this effect is greatest in water absorption bands at about 1.4, 1.9 and 2.7 μm (clay soils also have hydroxyl absorption bands at about 1.4 and 2.2 μm). Soil moisture content is strongly related to the soil texture: coarse, sandy soils are usually well drained, resulting in low moisture content and relatively high reflectance; poorly drained fine textured soils will generally have lower reflectance. In the absence of water, however, the soil itself will exhibit the reverse tendency: coarse textured soils will appear darker than fine textured soils. Thus, the reflectance properties of a soil and consistent only within particular ranges of conditions. Two other factors that reduce soil reflectance are surface roughness and content of organic matter. The presence of iron oxide in a soil will also significantly decrease reflectance, at least in the visible wavelengths. [1]

2.3.3.3 Spectral Reflectance of Water

The spectral reflectance of water, probably the most distinctive characteristic is the energy absorption at near-infrared wavelengths. In short, water absorbs energy in these wavelengths whether water features per se (such as lakes and streams) or water contained in vegetation or soil. Locating and delineating water bodies with remote sensing data are done most easily in near-infrared wavelenghts because of this absorption property. However, various conditions of water bodies manifest themselves primarily in visible wavelengths. The energy/matter interactions at these wavelengths are very complex and depend on a number of interrelated factors. For example, the reflectance from a water body can stem from an interaction with the water's surface (specular reflection), with material suspended in the water, or with the bottom of the water body. Even with deep water where bottom effects are negligible, the reflectance properties of a water body are not only a function of the water per se but also the material in the water.

Clear water absorbs relatively little energy having wavelengths less than about 0.6 μm. High transmittance typifies these wavelengths with a maximum in the blue-green portion of the spectrum. However, as the turbidity of water changes (because of the presence of organic or inorganic materials) transmittance-and therefore reflectance-changes dramatically. For example, water containing large quantities of suspended sediments resulting from soil erosion normally have much higher visible reflectance than other "clear" waters in the same geographic area. Likewise, the reflectance of water changes with the chlorophyll concentration involved. Increases in chlorophyll concentration tend to decrease water reflectance in blue wavelengths and increase it in green wavelengths. These changes have been used to monitor the presence and estimate the concentration of algae via remote sensing data. Reflectance data have also been used to determine the presence or absence of tanning dyes from bog vegetation in lowland areas, and to detect a number of pollutants, such as oil and certain industrial wastes.

Many important water characteristics, such as dissolved oxygen concentration, pH and salt concentration, cannot be observed directly through changes in water reflectance. However, such parameters sometimes correlate with observed reflectance. There are many complex interrelationships between the spectral reflectance of water and particular characteristics. [1]

3. SATELLITE SYSTEMS

A satellite with remote sensors to observe the earth is called a remote-sensing satellite, or earth observation satellite. [3] Remote sensing as a technology started with the first photographs in the early nineteenth century. Many significant events led to the launch of the Landsat satellites. [4] NASA began in the 1970s to build and launch Earth resource mapping satellites, the first of which was the Landsat series. Landsat 1, launched on July 23, 1972, as the Earth Resources Technology Satellite (ERTS) and later renamed. [23] After launching of Landsat satellites, other commercial remote sensing satellites began to take place in the developing remote sensing technologies.

3.1 NOAA / AVHRR Satellite System

The National Oceanic and Atmospheric Administration (NOAA) of the USA operates the series of NOAA satellites which each carry the Advanced Very High Resolution Radiometer (AVHRR) sensor. These sensors collect global data on a daily basis for a variety of land, ocean, and atmospheric applications. Specific applications include forest fire detection, vegetation analysis, weather analysis and forecasting, climate research and prediction, global sea surface temperature measurements, ocean dynamics research and search and rescue.

The first operational NOAA satellite (NOAA-6) was launched in 1979. This was followed by a series of additional NOAA satellites with the latest launch being NOAA-17 in June 2002. NOAA's 12, 15 and 16 are all still transmitting AVHRR data (Table 3.1).

The AVHRR sensor is a five or six channel (depending on the model) scanner, sensing the visible, near-infrared, and thermal infrared portions of the electromagnetic spectrum (Table 3.2). It provides global on board collection of data over a 2399 km swath. The sensor orbits the earth 14 times each day from an altitude of 833 km.

ACRES collects direct broadcast AVHRR data (ie. not recorded data) from within our acquisition circle several times every day. Prior to April 2002, only the afternoon passes from NOAA-16 were collected due to acquisition conflicts for the morning passes. During April 2002, a dedicated NOAA antenna was installed in Alice Springs permitting acquisition from NOAA's 12, 15, 16 and 17 from both day and night-time passes. There are normally about 2 day-time passes per satellite and 2 night-time passes per satellite. [11]

Table 3.1 NOAA-AVHRR sensor characteristics

Swath width	2399km
Spatial Resolution	1.1km approx.
Altitude	833km
Radiometric Resolution	10 bit
Orbit type	Sun synchronous
No. of orbits per day	14.1 (approx.)

Table 3.2 NOAA-AVHRR spectral characteristics

Channel No	**Wavelength**		**Typical use**
	NOAA-12 (µm)	**NOAA-15, 16, 17 (µm)**	
1	0.58 - 0.68	0.58 - 0.68	Daytime cloud and surface mapping
2	0.725 - 1.00	0.725 - 1.00	Land-water boundaries
3	3.55 - 3.93	N/A	Night cloud mapping, sea surface temperature
3A	N/A	1.58 - 1.64	Snow and ice detection
3B	N/A	3.55 - 3.93	Night cloud mapping, sea surface temperature
4	10.30 - 11.30	10.30 - 11.30	Night cloud mapping, sea surface temperature
5	11.50 - 12.50	11.50 - 12.50	Sea surface temperature

3.2 MODIS Satellite System

MODIS (Moderate Resolution Imaging Spectradiometer) is the key instrument aboard the satellites Terra (EOS AM-1), launched on 18 December 1999 and Aqua (EOS PM-1), launched on 4 May 2002.

MODIS views almost the entire surface of the Earth every day, acquiring data in 36 spectral bands over a 2330 km swath (Table 3.3).

MODIS data will improve the understanding of global dynamics and processes occurring on the land, in the oceans, and in the lower atmosphere (Table 3.4). MODIS is playing a vital role in the development of validated, global, interactive Earth system models able to predict global change accurately enough to assist policy makers in making sound decisions concerning the protection of our environment. [12]

Table 3.3 MODIS sensor characteristics

Swath width	2330 km (cross track) by 10 degrees of latitude (along track at nadir)
Spatial Resolution	250 m (bands 1-2) 500 m (bands 3-7) 1000 m (bands 8-36)
Altitude	705 km
Radiometric Resolution	12 bit
Orbit type	10:30 a.m. descending node (Terra) or 1:30 p.m. ascending node (Aqua), sun-synchronous, near-polar, circular

Table 3.4 MODIS spectral characteristics

Channel No	**Wavelength (μm)**	**Typical use**
1	0,620 – 0,670	Land/cloud/aerosols boundaries
2	0,841 – 0,876	
3	0,459 – 0,479	Land/cloud/aerosols properties
4	0,545 – 0,565	
5	1,230 – 1250	
6	1,628 – 1,652	
7	2,105 – 2,155	
8	405 – 420	Ocean color/phytoplankton/biochemistry
9	438 - 448	
10	483 - 493	
11	526 - 536	
12	646 - 556	
13	662 - 672	
14	673 - 683	
15	743 - 753	
16	862 - 877	
17	890 - 920	Atmospheric water vapor
18	931 – 941	
19	915 – 965	
20	3.660 - 3.840	Surface/cloud temperature
21	3.929 - 3.989	
22	3.929 - 3.989	
23	4.020 - 4.080	
24	4.433 - 4.080	Atmospheric temperature
25	4.482 - 4.549	
26	1.360 - 1.390	Cirrus clouds/water vapor
27	6.535 - 6.895	
28	7.175 - 7.475	
29	8.400 - 8.700	Cloud properties
30	9.580 - 9.880	Ozone
31	10.780 - 11.280	Surface/cloud temperature
32	11.770 - 12.270	
33	13.185 - 13.485	Cloud top altitude
34	13.485 - 13.785	
35	13.785 - 14.085	
36	14.085 - 14.385	

3.3 ENVISAT-MERIS Satellite System

Medium Resolution Imaging Spectrometer (MERIS) has been launched by the European Space Agency (ESA) onboard its polar orbiting Envisat Earth Observation Satellite (Table 3.5). MERIS, primarily dedicated to Ocean Colour Observations has in the past broadened its scope of objectives to atmospheric and land surface related studies. This is permitted by the large flexibility that sensor and ground segment provide.

MERIS has a high spectral and radiometric resolution and a dual spatial resolution, within a global mission covering open ocean and coastal zone waters and a regional mission covering land surfaces (Table 3.6). One of the most outstanding features of MERIS is the programmability of its spectral bands in their width and position.

The global mission of MERIS has a major contribution to scientific projects which seek to understand the role of the oceans and ocean productivity in the climate system through observations of water color and is furthering our ability to forecast change through models. Secondary objectives of the MERIS mission is directed to the understanding of atmospheric parameters associated with clouds, water vapor and aerosols in addition to land surface parameters, in particular vegetation processes.

MERIS is considered to be a remote sensing tool with a large potential to contribute to climate studies and global change observations in addressing environmental features in a multi-disciplinary way.

Table 3.5 ENVISAT-MERIS sensor characteristics

Swath width	1150 km
Spatial Resolution	300 m
Altitude	800 km
Radiometric Resolution	12 bit
Orbit type	Sun synchronous
Time for one orbit	101 minutes

Table 3.6 MERIS spectral characteristics

Channel No	Wavelength (µm)	Typical Use
1	0,413	Yellow substance and detrital pigments
2	0,443	Chlorophyll absorption maximum
3	0,490	Chlorophyll and other pigments
4	0,510	Suspended sediment, red tides
5	0,560	Chlorophyll absorption minimum
6	0,620	Suspended sediment
7	0,665	Chlorophyll absorption and fluo. reference
8	0,681	Chlorophyll fluorescence peak
9	0,709	Fluo. Reference, atmospheric corrections
10	0,754	Vegetation, cloud
11	0,761	Oxygen absorption R-branch
12	0,779	Atmosphere corrections
13	0,865	Vegetation, water vapour reference
14	0,885	Atmosphere corrections
15	0,900	Water vapour, land

3.4 LANDSAT Satellite System

The first Landsat satellite was launched in July 1972. Of the sensors carried, the Multispectral Scanner (MSS) with 80-metre pixels and four spectral bands was found to provide information of unforeseen value. In July 1982, the launch of Landsat 4 saw the inclusion of the Thematic Mapper (TM) sensor with a 30-metre resolution and 7 spectral bands. Both sensors are on Landsat 5 (Table 3.7).

The newest in this series of remote sensing satellites is Landsat 7. Launched on 15 April 1999, Landsat 7 has the new Enhanced Thematic Mapper Plus (ETM+) sensor. This sensor has the same 7 spectral bands as its predecessor, TM, but has an added panchromatic band with 15-metre resolution and a higher resolution thermal band of 60 meters (Table 3.8 and Table 3.9).

Table 3.7 Historical information of the LANDSAT satellites

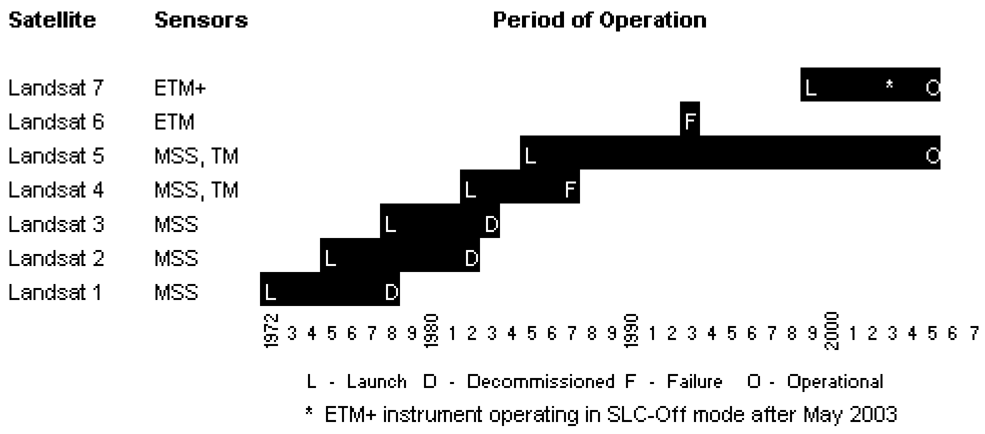

Table 3.8 LANDSAT ETM+ and TM sensor characteristics

		Landsat 7 ETM+	Landsat 5 TM
Swath width		185 km	185 km
Spatial Resolution	**Channels 1-5 & 7**	30 × 30 m	30 × 30 m
	Channel 6	60 × 60 m	120 × 120 m
	Channel 8	15 × 15 m pixel size (18 × 18 m GSI)*	N/A
Altitude		705 km	705 km
Radiometric Resolution		Best 8 of 9 bits	8 bits (256 levels)
Orbit type		Sun-synchronous Descending node: 10:00 am	Sun-synchronous Descending node: 10:10 am
Temporal Resolution		16 days (233 orbits)	16 days (233 orbits)
* ETM + channel 8 (panchromatic) was designed to be acquired at 15m resolution, but post-launch testing shows a ground sampling interval closer to 18m.			

Table 3.9 Spectral characteristics of the ETM+ and TM

Channel No	Wavelength (μm)	Typical Use
1	0.45 - 0.52	Coastal water mapping, differentiation of vegetation from soils
2	0.52 - 0.60	Assessment of vegetation vigour
3	0.63 - 0.69	Chlorophyll absorption for vegetation differentiation
4	0.76 - 0.90	Biomass surveys and delineation of water bodies
5	1.55 - 1.75	Vegetation and soil moisture measurements; differentiation between snow and cloud
6	10.40- 12.50	Thermal mapping, soil moisture studies and plant heat stress measurement
7	2.08 - 2.35	Hydrothermal mapping
8	0.52 - 0.90 (panchromatic)	Large area mapping, urban change studies

3.5 SPOT Satellite System

The development of Systeme Pour l'Observation de la Terre or SPOT program was undertaken by the French Government in 1978. Thereafter, Sweden and Belgium agreed to participate in the program with the aim of launching the first of a series of SPOT earth observation satellites. SPOT was designed as a commercially oriented program which was to be operational, rather than experimental, in character.

Conceived and designed by the French Centre National d'Etudes Spatiales (CNES), SPOT has developed into a large scale international program with ground receiving stations and data distribution outlets located in more than 30 countries. The first satellite in the program, SPOT-1, was launched from the Kourou Launch Range in French Guiana on February 21, 1986, onboard an Ariane launch vehicle. This satellite began a new era in space remote sensing, for it is the first earth resource satellite system to include a linear array sensor and employ push-broom scanning techniques. It is also the first system to have pointable optics. This enables side-to-side off-nadir viewing capabilities, and it affords full-scene stereoscopic imaging from two different satellite tracks permitting coverage of the same area. [1]

SPOT 1, 2, & 3 are the first three satellites were identical and their payloads consisted of two identical HRV (Visible High-Resolution) optical instruments, data recorders (on magnetic tapes), and a system for transmitting the images to the ground-based receiving stations (downlink).

SPOT 4 is the second most recent addition to the SPOT family is an enhancement of the earlier versions. Its payload consists of several sensors (two identical HRVIR (Visible & Infrared High-Resolution) optical sensors and the VEGETATION sensor), data recorders (on magnetic tapes), and a system for transmitting the images to the ground-based receiving stations (downlink).

SPOT 5 has high resolution imaging instruments delivering these product improvements:

- dedicated instrument for along track stereo acquisition,
- higher ground resolution: 5 metres and 2.5 metres (instead of 10 m) in panchromatic mode,
- higher resolution in multispectral mode: 10 m (instead of 20 m) in all 3 spectral bands in the visible and near infrared ranges.

The spectral band in the short wave infrared band (essential for VEGETATION data) is maintained at a resolution of 20 m due to limitations imposed by the geometry of the CCD sensors used in this band.

The field width of each instrument: 60 km, same as Spot 1, 2, 3 and 4. The oblique viewing capacity of each instrument is maintained providing rapid access to a given area. SPOT products differ by pixel size (ground sample distance of 2.5 m, 5 m, 10 m or 20 m) and spectral acquisition mode (black and white or colour). [22]

Table 3.11 shows sensor characteristics of SPOT Satellites and Table 3.12 shows spectral characteristics of the SPOT Sensors.

VEGETATION Sensor

The VEGETATION programme is co-financed by the European Union, Belgium, France, Italy, and Sweden and being conducted under the supervision of the CNES. The aim of the VEGETATION instrument is to provide accurate measurements of the main characteristics of the Earth's plant cover. Practically daily global coverage and a resolution of 1 kilometre make this sensor an ideal tool for observing long-term regional and global environmental changes.

VEGETATION works independently from the HRVIRs. It includes a wide-angle radiometric 'camera' operating in four spectral bands (blue, red, near-infrared, and middle-infrared) at a resolution of 1 km (Table 3.10). Given its 2,250km swaths, this instrument is thus able to cover almost all of the Earth's dry land in just one day. [22]

Table 3.10 VEGETATION sensor & spectral characteristics

Channel No	Wavelength (µm)	Spatial Resolution
B0	0,43 - 0,47	1165m x 1165m
B2	0,61 - 0,68	1165m x 1165m
B3	0,79 - 0,89	1165m x 1165m
MIR	1,58 - 1,75	1165m x 1165m

Table 3.11 SPOT sensor characteristics

	SPOT 1,2,3 HRV Sensor	SPOT 4 HRVIR Sensor Vegetation Sensor	SPOT 5 HRG&HRS Sensor Vegetation 2 Sensor
Swath width	60 km	60 km	60 km
Spatial Resolution	20 m (MS) 10 m (P)	20 m (MS) 10 m (P)	10 m (MS) 20 m (SWIR) 5 m and 2.5 m (P)
Altitude	822 km	830 km	832 km
Radiometric Resolution	8 bit	8 bit	8 bit
Orbit type	Sun synchronous polar	Sun synchronous polar	Sun synchronous polar
HRV: Visible High Resolution HRVIR: Visible & Infrared High Resolution HRG: High Resolution Geometric HRS: High Resolution Stereopair			

Table 3.12 SPOT spectral characteristics

Channel No	Wavelength (µm)			Typical Use
	SPOT 1, 2, 3	SPOT 4	SPOT 5	
1	0,50 - 0,59	0,50 - 0,59	0,50 - 0,59	Recommended for use in combination with other bands because of low contrast and sensitivity to haze
2	0,61 - 0,68	0,61 - 0,68	0,61 - 0,68	Best for showing roads and bare soils. This band heightens the contrast between vegetated and non-vegetated areas
3	0,79 - 0,89	0,79 - 0,89	0,79 - 0,89	This band is used to evaluate vegetation biomass and separates water from vegetation.
4	-	1,58 - 1,75	1,58 - 1,75	This band is used to monitor soil water content and forest (clear cut mapping, timber volume etc.)
Panchromatic (P)	0,51 - 0,73	0,61 - 0,68	0,51 - 0,73	This band is intended primarily for applications calling for fine geometrical detail

4. DIGITAL IMAGE PROCESSING

Image processing and analysis can be defined as the "act of examining images for the purpose of identifying objects and judging their significance". Image analyst study the remotely sensed data and attempt through logical process in detecting, identifying, classifying, measuring and evaluating the significance of physical and cultural objects, their patterns and spatial relationship. [3]

4.1 Digital Image

Remote sensing images are recorded in digital forms and then processed by the computers to produce images for interpretation purposes. In a most generalized way, a digital image is an array of numbers depicting spatial distribution of a certain field parameters (such as reflectivity of EM radiation, emissivity, temperature or some geophysical or topographical elevation). Digital image consists of discrete picture elements called pixels. Associated with each pixel is a number represented as DN (Digital Number), that depicts the average radiance of relatively small area within a scene. The range of DN values being normally 0 to 255. [3]

All of the pictures, which are viewed on the computer, are 8-bit digital images, which mean that they have 256 colors (2^8). Digital images are tables of numbers, which in this case range from 0 to 255. In Figure 4.1, the "bright" squares (called pixels) have high number values (ie. 200 to 255), while the "dark" pixels, have low number values (ie. 0-100). The satellite sensor records the reflectance in its field of view, and then scales the signal to an 8-bit number (0 to 255). [21]

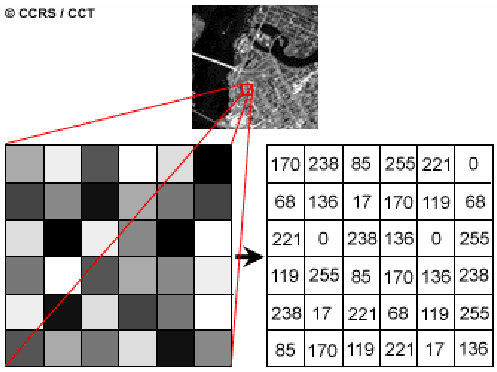

Figure 4.1 Digital image [2]

4.1.1 Image Resolution

Resolution can be defined as "the ability of an imaging system to record fine details in a distinguishable manner". A working knowledge of resolution is essential for understanding both practical and conceptual details of remote sensing. [3] The major characteristics of imaging remote sensing instrument operating in the visible and infrared spectral region are described in terms as follow:

- Spectral resolution
- Radiometric resolution
- Spatial resolution
- Temporal resolution

4.1.1.1 Spectral Resolution

This type of resolution refers to the number and width of channels of an instrument samples within the electromagnetic spectrum. Different materials on the earth surface have different spectral reflectances and emissivities. These spectral characteristics define the spectral position and spectral sensitivity in order to distinguish materials. The use of well-chosen and sufficiently numerous spectral bands is a necessity, therefore, if different targets are to be successfully identified on remotely sensed images. [3] In Figure 4.2, image of Salt Lake is taken with 4 spectral channels of SPOT XI sensor.

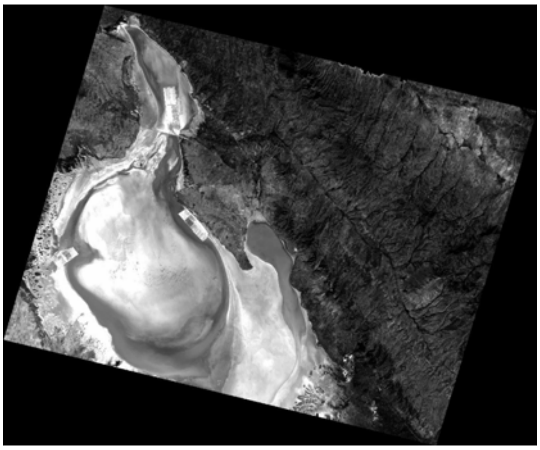

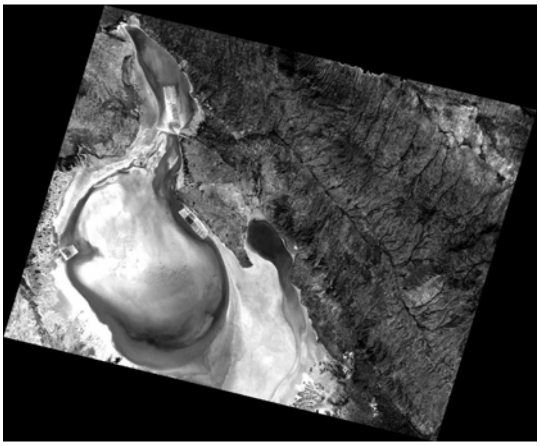

Channel 1 **Channel 2**

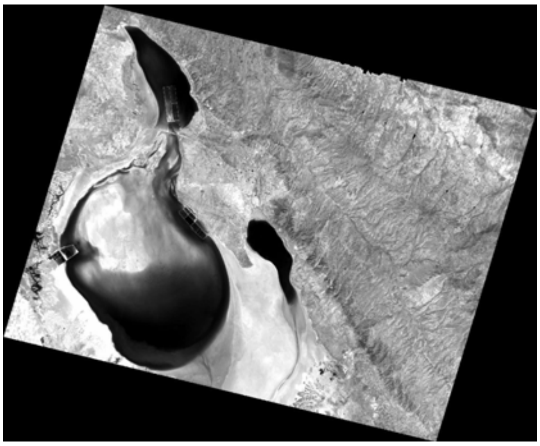

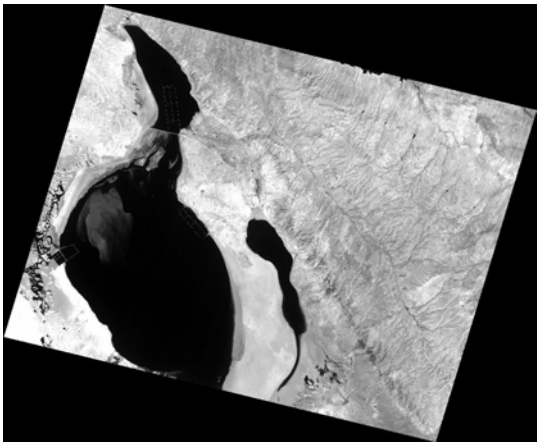

Channel 3 **Channel 4**

Figure 4.2 Channels of SPOT XI sensor

4.1.1.2 Radiometric Resolution

Radiometric Resolution or radiometric sensitivity refers to the number of digital levels used to express the data collected by the sensor. It is commonly expressed as the number of bits. [3] In Figure 4.3, there are a low and a high radiometric resolution image of the same area.

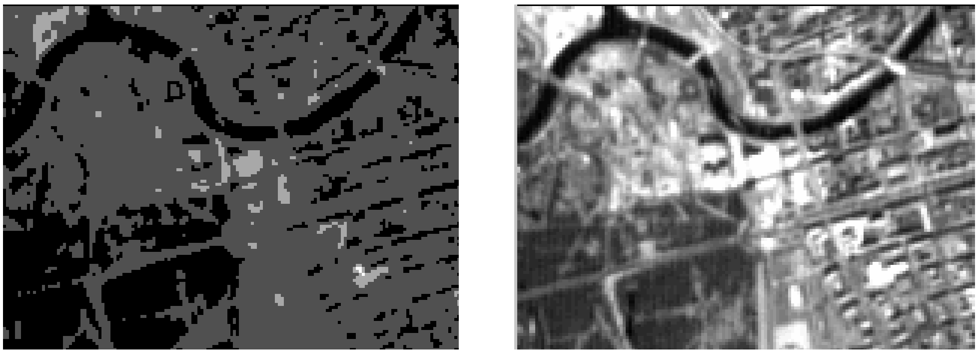

(a) 2 bit (b) 8 bit

Figure 4.3 Low (a) and high (b) radiometric resolutions [27]

4.1.1.3 Spatial Resolution

The detail discernible in an image is dependent on the spatial resolution of the sensor and refers to the size of the smallest possible feature that can be detected. Commercial satellites provide imagery with resolutions varying from several centimetres to kilometres. The finer the resolution, the less total ground area can be seen (Figure 4.4). Images where only large features are visible are said to have coarse or low resolution. In fine or high resolution images, small objects can be detected. Military and some commercial sensors for example, are designed to view as much detail as possible, and therefore have very fine resolution. [2]

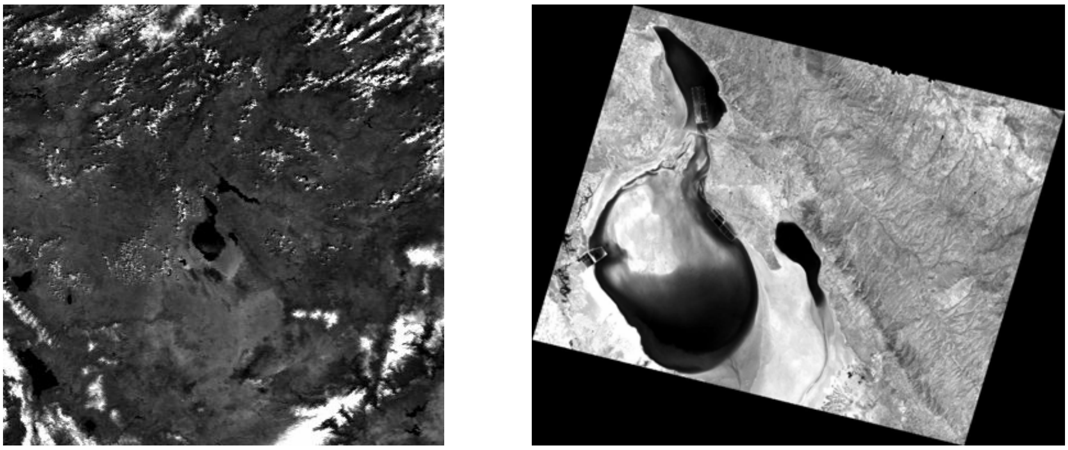

Low spatial resolution (1.1 km) (NOAA-AVHRR image)

High spatial resolution (20 m) (SPOT-XI image)

Figure 4.4 Low and high spatial resolutions

It is important to distinguish between pixel size and spatial resolution - they are not interchangeable. If a sensor has a spatial resolution of 20 metres and an image from that sensor is displayed at full resolution, each pixel represents an area of 20m x 20m on the ground. In this case the pixel size and resolution are the same. However, it is possible to display an image with a pixel size different than the resolution. Many posters of satellite images of the Earth have their pixels averaged to represent larger areas, although the original spatial resolution of the sensor that collected the imagery remains the same. [2] In Figure 4.5, there are several images of the same area in different spatial resolution.

10 meter resolution   30 meter resolution   80 meter resolution

Figure 4.5 Different spatial resolution images of the same area [29]

4.1.1.4 Temporal resolution

Temporal resolution is the period of elapsed time between images taken of the same object at the same location. The more frequent a sensor is able to return to an exact specific location the greater the temporal resolution. Several observations over time reveal changes and variations in the object being observed. For satellite systems temporal resolution is described as the revisit period, which refers to the time it takes for a satellite to return to the same area on subsequent orbits. [34]

The ability to collect imagery of the same area of the Earth's surface at different periods of time is one of the most important elements for applying remote sensing data. Spectral characteristics of features may change over time and these changes can be detected by collecting and comparing multi-temporal imagery (Figure 4.6). [2]

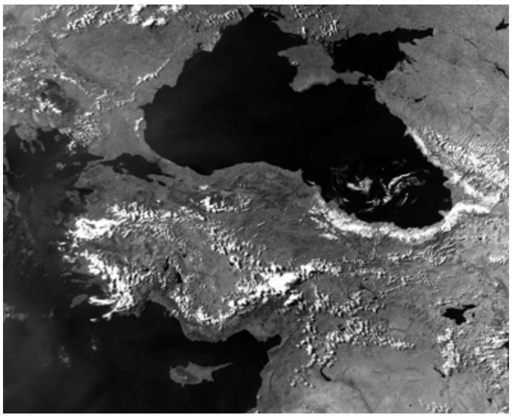

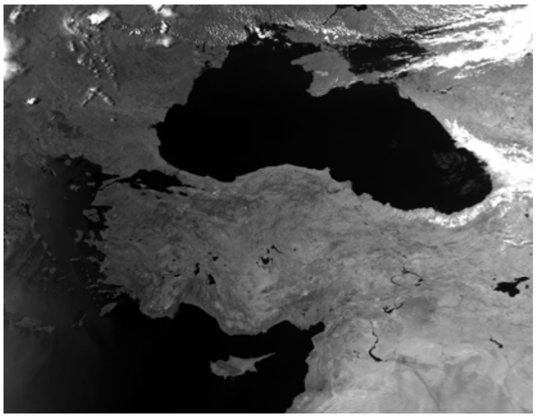

22 June 2002 NOAA-2/band2 13 June 2000 NOAA-2/band2

2 March 2000 NOAA-2/band 2

Figure 4.6 An example for temproral resolution

4.2 Preprocessing

Preprocessing is an important and diverse set of image preparation programs that act to offset problems with the band data and recalculate DN values that minimize these problems. Among the programs that optimize these values are atmospheric correction (affecting the DNs of surface materials because of radiance from the atmosphere itself, involving attenuation and scattering); sun illumination geometry; surface-induced geometric distortions; spacecraft velocity and altitude variations; effects of Earth rotation, elevation, curvature, abnormalities of instrument performance (irregularities of detector response and scan mode such as variations in mirror oscillations); loss of specific scan lines and others. Once performed on the raw data, these adjustments require appropriate radiometric and geometric corrections. [4]

4.2.1 Image restoration

4.2.1.1 Radiometric Correction

Image radiometry is affected by factors, such as system noise, sensor malfunction and atmospheric interference. The purpose of radiometric correction is to remove or reduce the sensor inconsistencies, sensor malfunction, viewing geometry and atmospheric effects. [35]

4.2.1.2 Geometric Correction

Registiration/Rectification

Geometric correction is undertaken to avoid geometric distortions from a raw image, and is achieved by establishing the relationship between the image coordinate system and the geographic coordinate system using ground control points (Figure 4.7). When the image coordinates of the points in the slave image match to their true positions in ground coordinates (i.e. lattitude, longtitude), the process is called rectification, and when this process is done as image-to-image application it is called registration (i.e. for image merging). [25]

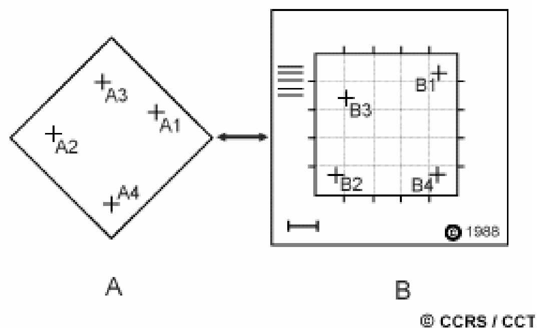

Figure 4.7 Registiration Process [2]

Steps of Rectification

Registration and Rectification involve similar sets of procedures. Steps which explain below are also applied image-to-image registiration.

1. Ground control points are located.
2. A transformation matrix is computed and tested.
3. An output image file with the new coordinate information in the header is created. The pixels must be resampled to conform to the new grid.

Ground control points

Ground control points (GCP's) are specific pixels in an image for which the output map coordinates (or other output coordinates) are known. GCP's consist of two X,Y pairs of coordinates:

- source coordinates- usually data file coordinates in the image being rectified.
- Reference coordinates- the cordinates of the map or reference image to which the source image is being rectified.

Entering GCPs

Accurate ground control points are essential for an accurate rectification. From the ground control points, the rectified coordinates for all other points in the image are extrapolated. Many GCP's throughout the scene are selected. The more dispersed the GCP's are, the more reliable the rectification will be. GCP's for large-scale imagery might include the intersection of two roads, airport runways, utility corridors, towers, or buildings. For small-scale imagery, larger features such as urban areas or geologic features may be used. Landmarks that can vary, such as the edges of lakes or other water bodies, vegetation, etc. should not be used as GCP's. [24]

Orders of transformation

Polynomial equations are used to convert source file coordinates to rectified map coordinates. Depending upon the distortion in the imagery, the number of GCP's used, and their locations relative to one another, complex polynomial equations may be required to express the needed transformation. The degree of complexity of the polynomial is expressed as the order of the polynomial. The order is simply the highest exponent used in the polynomial. [24]

Transformation matrix

A transformation matrix is computed from the GCP's. The matrix consist of coefficients which are used in polynomial equations to convert the coordinates. The size of matrix depends upon the order of transformation. The goal in calculating the coefficients of the transformation matrix is to derive the polynomial equations for which there is the least possible amount of error when they are used to transform the reference coordinates of the GCP's into the source coordinates. [24]

Linear tranformations

A 1-st order transformation is a linear transformation. First-order transformations can be used to project raw imagery to a planar map projection, convert a planar map projection to another planar map projection, and when rectifying relatively small image areas.

Nonlinear transformations

Transformations of the 2nd-order or higher are nonlinear transformations. This transformations can correct nonlinear distortions. Second-order transformations can be used to convert Lattitude/Longitude data to a planar projection, for a data covering a large area (to account for the earth's curvature) with distorted data (for example, due to camera lens distortion). Third-order transformations are used with distorted aerial photographs, on scans of warped and with radar imagery. Fourth-order transformations can be used on very distorted aerial photographs. [24]

Minumum number of GCP's

Higher orders of transformations can be used to correct more complicated types of distortion. However, to use a higher order of transformation, more GCP's are needed. For instance, three points define a plane. Therefore, to perform a 1-st order transformation, which is expressed by the equation of a plane, at least three GCP's are needed. Similary, the equation used in 2nd-order transformation is the equation of a paraboloid. Six points are required to define a paraboloid. Therefore, at least six GCP's are required to perform a 2nd-order transformation. The minumum number of points required to perform a transformation of order t equals:

$$((t+1)*(t+2))/2$$

GCP's should be used more than the minumum number whenever possible.

In most cases, a perfect fit all GCP's would require an unnecessarily high order of transformation. Instead of increasing the order, there is an option to tolerate a certain amount of error. When a transformation matrix is calculated, the inverse of the transformation matrix is used to transform the reference coordinates of GCP's back to the source coordinate system.

RMS error(root mean square) is the distance between the input(source) location of a GCP, and the retransformed location for the same GCP. In other words, it is the difference between the desired output coordinate for a GCP and the actual output coordinate for the same point when the point is transformed with the transformation matrix.

RMS error is calculated with a distance equation:

$$\text{RMS error}=\sqrt{(x_r-x_i)^2+(y_r-y_i)^2}$$

Where:

x_i and y_i are the input source coordinates.

x_r and y_r are the retransformed coordinates.

An RMS error of 2 means that the reference pixel is 2 pixels away from the retransformed pixel. [24]

Resampling

In order to actually geometrically correct the original distorted image, a procedure called resampling is used to determine the digital values to place in the new pixel locations of the corrected output image. The resampling process calculates the new pixel values from the original digital pixel values in the uncorrected image. [2] There are three common methods for resampling: nearest neighbour, bilinear interpolation, and cubic convolution. In nearest neighbour method, the nearest point will be sampled (Figure 4.8). The geometric error will be a half pixel at maximum. It has the advantage of being easy and fast. [31]

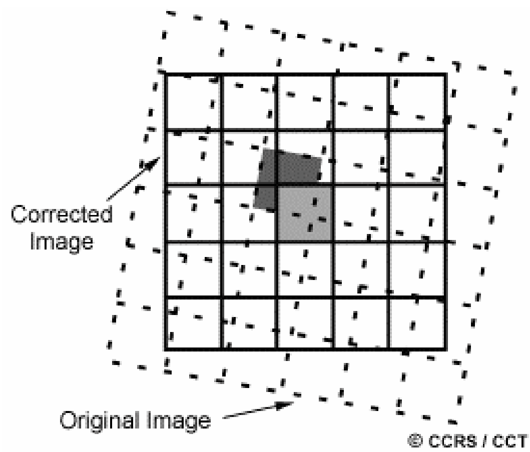

Figure 4.8 Nearest neighbour method [2]

Bilinear interpolation method is applied to the surrounding four points (Figure 4.9). The spectral data will be smoothed after the interpolation. [31]

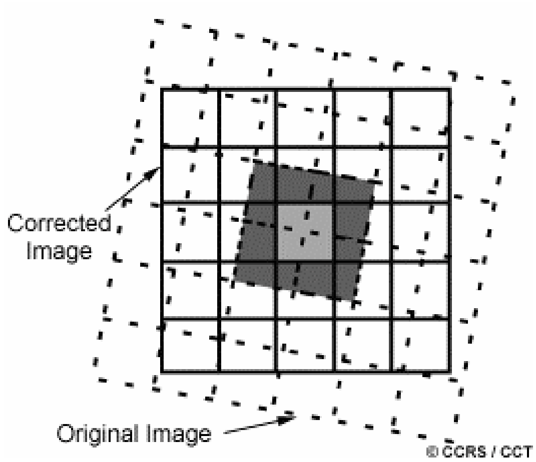

Figure 4.9 Bilinear interpolation method [2]

The spectral data will be interpolated by cubic convolution using the surrounding sixteen points (Figure 4.10). The cubic convolution results in sharpening as well as smoothing, though the computation takes a longer time when compared with the other methods. [31]

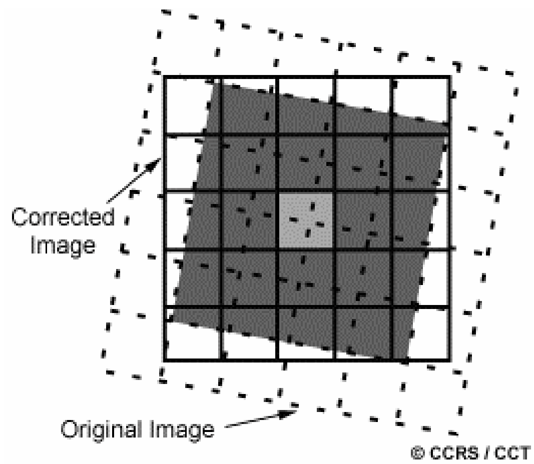

Figure 4.10 Cubic convolution method [2]

4.2.2 Image Enhancement

The goal of image enhancement is to improve the visual interpretability of an image by increasing the apparent distinction between the features in the scene. The process of visually interpreting digitally enhanced imagery attempts to optimize the complementary abilities of the human mind and the computer. The mind is excellent at interpreting spatial attributes on an image are capable of selectively identifying obscure or subtle features. However, the eye is poor at discriminating the slight radiometric or spectral differences that may characterize such features. Computer enhancement aims to visually amplify these slight differences to make them readily observable. [1]

Enhancement operations are normally applied to image data after the appropriate restoration procedures have been performed. Contrast enhancement, filtering, image ratio, density slicing are some of digital enhancement techniques.

4.2.2.1 Contrast Enhancement

Image display and recording devices typically operate over a range of 256 gray levels. Sensor data in a single image rarely extend over this entire range. Hence, the intent of contrast enhancement is to expand the narrow range of brightness values typically present in an input image over a wider range of gray values. [1]
There are many different techniques and methods of enhancing contrast and detail in an image. The simplest type of enhancement is linear contrast stretch (Figure 4.11).

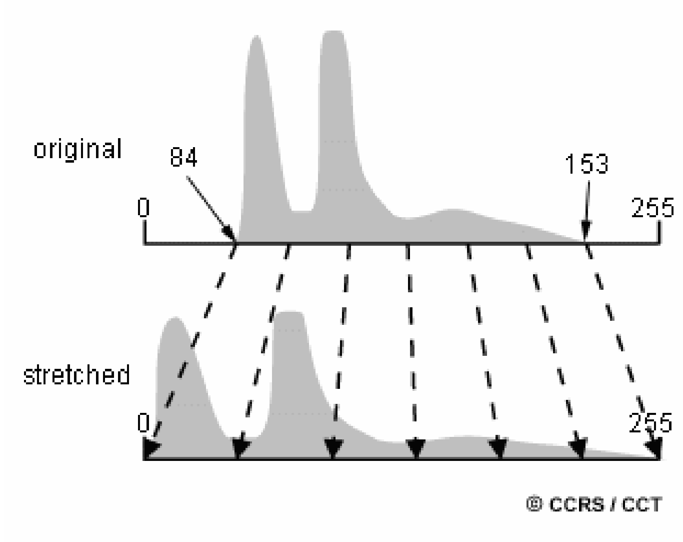

Figure 4.11 Linear contrast stretch [2]

Nonlinear contrast enhancement often involves histogram equalizations through the use of an algorithm. The nonlinear contrast stretch method has one major disadvantage. Each value in the input image can have several values in the output image, so that objects in the original scene lose their correct relative brightness values. [36]

Histogram equalization is one of the most useful forms of nonlinear contrast enhancement. When an image's histogram is equalized, all pixel values of the image are redistributed so there are approximately an equal number of pixels to each of the user-specified output gray-scale classes. Contrast is increased at the most populated range of brightness values of the histogram. It automatically reduces the contrast in very light or dark parts of the image associated with the tails of a normally distributed histogram. Histogram equalization can also seperate pixels into distinct groups, if there are few output values over a wide range.

4.2.3 Image Classification

Digital image classification uses the spectral information represented by the digital numbers in one or more spectral bands, and attempts to classify each individual pixel based on this spectral information (Figure 4.12). This type of classification is termed spectral pattern recognition. In either case, the objective is to assign all pixels in the image to particular classes or themes (e.g. water, coniferous forest, deciduous forest, corn, wheat, etc.). The resulting classified image is comprised of a mosaic of pixels, each of which belong to a particular theme, and is essentially a thematic "map" of the original image. [2]

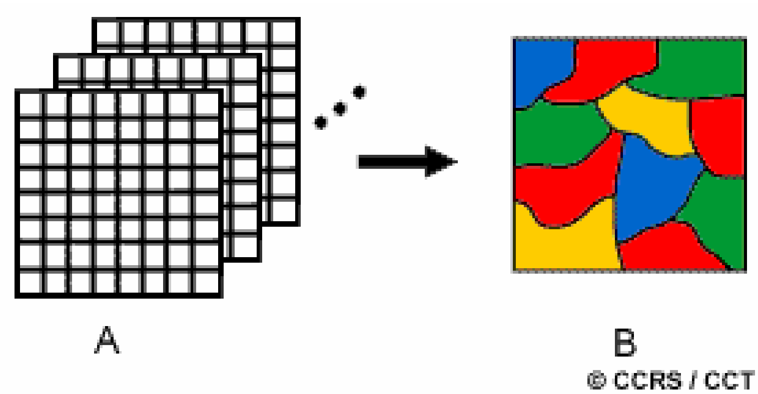

Figure 4.12 Image classification [2]

Common classification procedures can be broken down into two broad subdivisions based on the method used: supervised classification and unsupervised classification.

4.2.3.1 Supervised Classification

In a supervised classification, the analyst identifies in the imagery homogeneous representative samples of the different surface cover types (information classes) of interest. These samples are referred to as training areas. The selection of appropriate training areas is based on the analyst's familiarity with the geographical area and their knowledge of the actual surface cover types present in the image. Thus, the analyst is "supervising" the categorization of a set of specific classes. The numerical information in all spectral bands for the pixels comprising these areas is used to "train" the computer to recognize spectrally similar areas for each class. The computer uses a special program or algorithm, to determine the numerical "signatures" for each training class. Once the computer has determined the signatures for each class, each pixel in the image is compared to these signatures and labeled as the class it most closely "resembles" digitally (Figure 4.13). Thus, in a supervised classification we are first identifying the information classes, which are then used to determine the spectral classes, which represent them. [2]

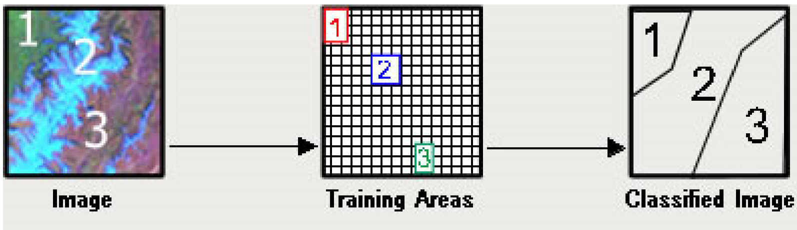

Figure 4.13 Supervised classification [25]

4.2.3.2 Unsupervised Classification

Unsupervised classification in essence reverses the supervised classification process. Spectral classes are grouped first, based solely on the numerical information in the data, and are then matched by the analyst to information classes. Programs, called clustering algorithms, are used to determine the natural groupings or structures in the data. Usually, the analyst specifies how many groups or clusters are to be looked for in the data. In addition to specifying the desired number of classes, the analyst may also specify parameters related to the separation distance among the clusters and the variation within each cluster. The final result of this iterative clustering process may result in some clusters that the analyst will want to subsequently combine, or clusters that should be broken down further - each of these requiring a further application of the clustering algorithm (Figure 4.14). Thus, unsupervised classification is not completely without human intervention. However, it does not start with a pre-determined set of classes as in a supervised classification. [2]

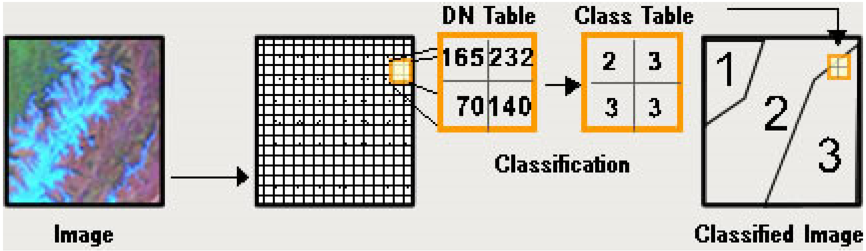

Figure 4.14 Unsupervised classification [25]

4.2.3.3 Digitizing Method

On-screen digitizing, or heads-up digitizing as it is sometimes called, is a manual method for creating land cover change maps, relying on visual interpretation. For this method, an analyst draws polygons representing the land cover change classes on a computer screen. This is the most subjective of the all approaches, and in some ways that is its greatest strength and weakness. It is strength because the human brain is still better at classifying the vast array of landscape features than a computer algorithm. The downside is that this approach is more susceptible to operator fatigue and bias than automated methods, and it tends to be slower in complex or large areas. [16]

4.2.3.4 Segmentation Method

Image segmentation is not a classification tool; rather, it is a method to group contiguous pixels into areas (segments) that are relatively homogeneous. It can be thought of as a preprocessing step before classifying an image. The segmentation is done using sophisticated algorithms that compare a pixel's value with the values of the neighboring pixels. If neighboring pixels are relatively similar then they are added to the contiguous group and if they are not then another segment is started. These programs provide variables that allow an analyst to specify the relative size and sometimes even the shape of the segments.

Once an image has been segmented it can be classified at the segment level instead of the pixel level. There are several advantages to this approach:

- it runs much faster since the number of segments is much less than the number of pixels in an image,
- the relative scale of the segmentation output can be specified so different segmentation runs can be used to capture features of different sizes,
- the classification algorithm can utilize the spectral characteristics (the pixel values) of an image as well as a host of other segment characteristics that describe the segment, such as mean pixel value, standard deviation, shape of the segments, and dimensions of the segment, and
- the resulting image does not suffer from the "salt and pepper" effect common to the pixel-by-pixel classifiers. [16]

5. APPLICATION

Salt Lake being the second largest lake in Turkey is a very important source of salt for Turkey. Since covering very large area in winter and not freezing even coldest days, it is an important area for aquatic birds to spend their winter time. Salt Lake is also declared as an “A class water area” according to International criteria. Hence, the changes in areal extent of Salt Lake is important both for aquatic birds habitat and also the ecosystem of the lake. In this study, NOAA-AVHRR (dated between 1997-2004) and SPOT XS/XI (dated 2005) images were processed to evaluate the temporal and annual changes in the lake.

5.1 Study Area

Salt Lake (38 45’N 33 23’E) is the second largest lake in Turkey (Figure 5.1). Its extent varies greatly with a maximum depth in spring of 1.5 m and most of the lake drying up in summer. The area receives the lowest annual precipitation in Turkey. The lake is fed by two major streams, groundwater and surface water. An unnaturally constant input is the waste water which reaches the lake through the 150 km-long Konya drain. Brackish marshes have formed where channels and streams enter the lake, and the lake is surrounded by (only partially irrigated) cereal fields in the north, east and west, whilst extensive seasonally-flooded salt-steppe occur, particularly to the south-west.

Salt Lake is extremely saline with a salt ratio of 32% (Figure 5.2). The lake bottom is covered with a 1-30 cm thick salt layer, which has given rise to a local salt industry providing 55% of all Turkish salt. [15]

Figure 5.1 Physical map of the study area [15]

Figure 5.2 An image from Salt Lake [26]

5.1.1 Conservation Issues

Salt Lake was declared as a Specially Protected Area (SPA) in 1992 (Figure 5.3). [15] Coordinates of Salt Lake-Specially Protected Area boundaries are given in Table 5.1. Decision, about these boundaries, with 2000/1381 number was published in Official Journal with 2.11.2000/24218 number. [32]

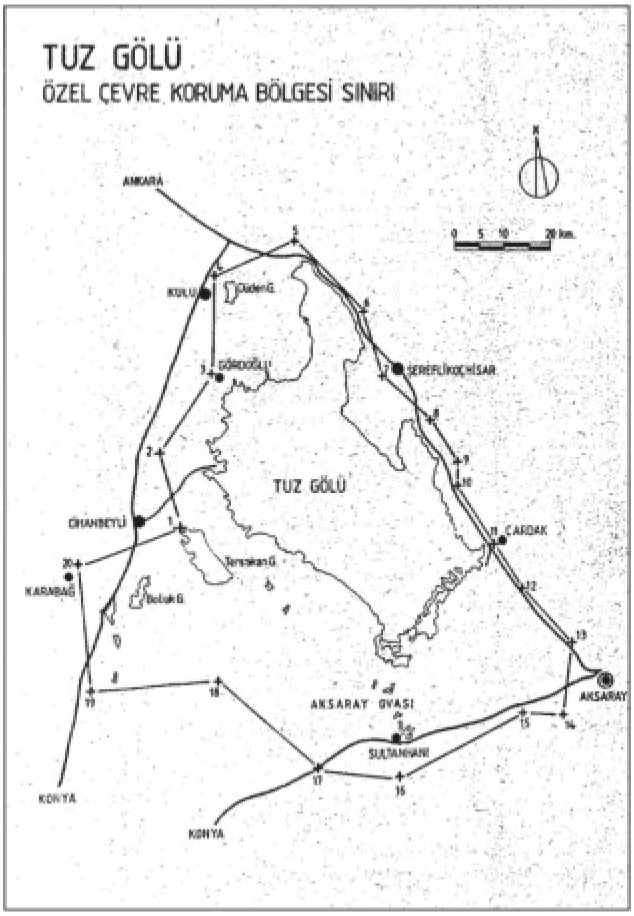

Figure 5.3 Specially Protected Area Boundaries [32]

Table 5.1 Coordinates of Salt Lake-Specially Protected Area boundaries [32]

Point No	Longitude	Latitude	Point No	Longitude	Latitude
1	33° 03' 10"	38° 40' 20"	11	33° 46' 44"	38° 36' 40"
2	32° 57' 02"	38° 17' 39"	12	33° 50' 03"	38° 32' 06"
3	33° 06' 04"	38° 56' 06"	13	33° 57' 50"	38° 25' 23"
4	33° 06' 14"	39° 06' 47"	14	33° 56' 42"	38° 17' 31"
5	33° 17' 56"	39° 11' 06"	15	33° 50' 53"	38° 17' 49"
6	33° 27' 54"	39° 02' 49"	16	33° 33' 57"	38° 11' 48"
7	33° 31' 23"	38° 55' 05"	17	33° 21' 59"	38° 12' 34"
8	33° 37' 44"	38° 50' 06"	18	33° 05' 56"	38° 21' 58"
9	33° 41' 13"	38° 45' 47"	19	33° 48' 22"	38° 20' 06"
10	33° 41' 06"	38° 42' 25"	20	33° 47' 06"	38° 33' 58"

As indicated by the report done by World Wildlife Fund (WWF);

- Salt Lake holds the main Turkish breeding colony of Greater Flamingo which breed on a group of islands in the southern part of the lake. Lesser Kestrel is a common breeder in villages around the lake. Avocet and Greater Sand plover also breed. During winter White-fronted Geese occur. Consequently, Salt Lake is an Important Bird Area (IBA) (Figure 5.4).

Figure 5.4 Salt Lake and other IBA's (Important Bird Area) [15]

- The main channel (completed in 1974) which drains the entire Konya irrigation area (IBA no. 67, 68 and 69) is 150 km-long and runs north from the irrigation area by-passing two other IBAs (Bolluk Lake [IBA no. 70] and Tersakan Lake [IBA no. 71]) before flowing into Salt Lake just 10 km from the flamingo breeding islands. All untreated sewage from Konya city (1 million inhabitants) and several hundreds of industries are released into the channel. Agricultural waste, which flows through the channel, includes pesticides and fertilizers used in the Konya basin. Industrial waste includes that from diary farms, aluminum and copper plants, leather processing units and a LPG bottling plant. Prevailing currents mean that most pollutants and sediment are deposited in the southern part of the lake, and the salines have not yet reported major pollution problems. Increasing pollution from rapidly growing Konya, its expanding industries and the increase in agricultural waste as more land in the Konya plain is irrigated, will place huge strains on Salt Lake.

- Exacerbating the effects of the pollution is the reduced input of clean water as a result of the construction of the Mamasın reservoir and the Cihanbeyli reservoir on the main inflows.
- Due to poor soils and a lack of water, no immediate plans for large scale intensification of agriculture in the direct surroundings of Salt Lake exist. Large tracts of (salt) steppe have been converted by individual farmers to arable land, principally for cereal production, over the years. To preserve the remaining steppe areas around Salt Lake, it is recommended that further agricultural intensification be immediately halted. [15]
- Despite its size, and also the rapid growth in demand for natural gas, Turkey currently has no natural gas storage capacity. The World Bank’s Gas Sector Development Project, will finance the construction of an underground natural gas storage facility and two key compressor stations. The underground storage facility will be built in an underground salt formation south of the Salt Lake. [33]

  Although this technology proposed has been successfully employed in the world, its effects to the Salt Lake are also considered another environmental issue.

5.2 Satellite Images Used

In this study, NOAA-AVHRR and SPOT XS/XI images were used and processed by the image processing software Envi 3.6. Images and its dates are given in Table 5.2.

Table 5.2 Satellite images used

Date	NOAA image
February 8,2001	N14h1333.039
February 8, 2004	ITU-CSCRS-2
March 2,2000	N14h1318.062
March 14,2000	N14h1242.074
March 10, 2001	N12h1405.069
March 1, 2004	ITU-CSCRS-1
April 6,2000	N14h1318.097
April 29,2001	N14h1427.119
May 10,1997	N14h1115.130
May 24,2001	N14h1429.144
May 31,2001	N14h1446.151
May 25,2002	N14h1540.145
May 19,2002	N15h1627.139
June 13,2000	N14h1335.165
June 12,2001	N14h1403.163
July 8,2000	N14h1346.190
July 29,2000	N14h1303.211
July 11,2001	N14h1458.192
July 7,2002	N14h1508.188
July 4,2002	N14h1545.185
August 7,2000	N14h1258.220
August 14,2000	N14h1317.227
August 15, 2001	N15h1601.239
August 12,2002	N15h0531.224
September 17,2001	N14h1246
September 7,2002	N15h0527.250
September 17,2002	N15h1611.187
October 31,1999	N14h1314.304
October 5,2000	N14h1312.279
November 3,1999	N14h1240.307
November15, 2000	N14h1333.320
December 17, 1999	N14h1242.351
Date	**SPOT image**
August 18, 2005	Spot-2
March 24, 2005	Spot-4

5.3 Image Processing

5.3.1 Preprocessing

As a first step, NOAA-AVHRR images were imported with ERDAS imagine software into ".img" file format. Radiometric correction option were used while importing into ".img" file format. In the radiometric correction phase, radiometric calibration using slope and intercept values for each band and sun angle correction were considered. The slope and intercept coefficients gathered from the satellite ephemeris, were applied to the pixel values to reduce the effect of natural variations in sensor response for images collected at different points in time. Sun angle correction was applied to the visible bands. This is done by applying a basic correction formula (1/cosine({sun angle})) to the pixel values.

Since the images cover a very broad area including Turkey and some part of Europe, the area covering Turkey was cropped from all images used. However, 10 of 60 images were cloudy and 18 of 60 images were distorted. Therefore, these images weren't used in this study (Figure 5.5 and 5.6).

Figure 5.5 An example of a cloudy image (22 June 2002, NOAA-14/band 2)

(a) 17 September 2002, NOAA-14/band 3

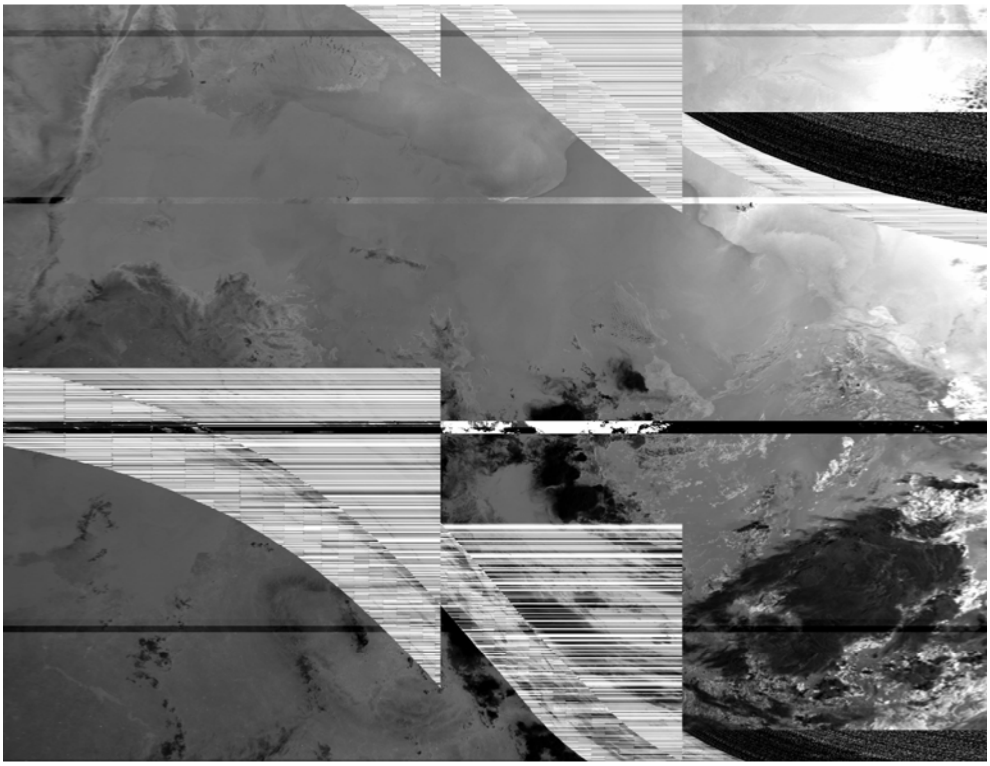

(b) 27 August 2002, NOAA-14/band 3

Figure 5.6 Examples of distorted images

5.3.2 Image Rectification

Since NOAA images were very distorted, all NOAA images were rectified with using second order polynomial transformation. As a first step, several well-distributed GCP (Ground Control Points) pairs were identified (Figure 5.7). RMS (Root Mean Square) error was taken as ±1.0. GCP numbers and rms errors are given in Table 5.3 for every image used.

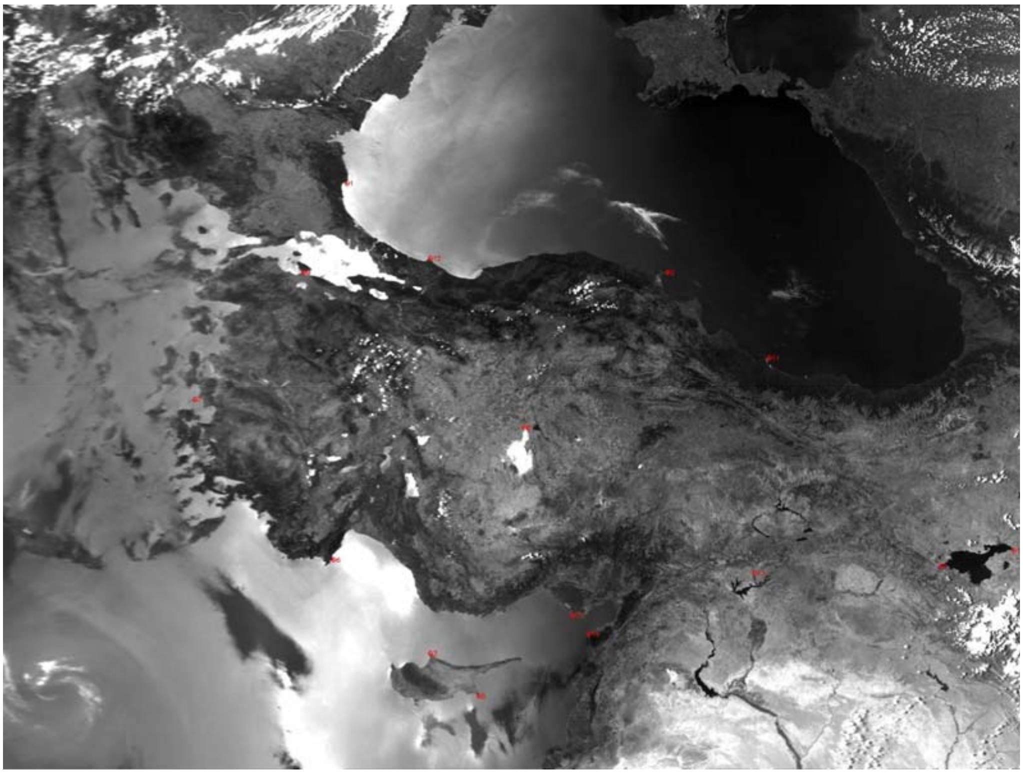

Figure 5.7 GCP’s selected for the rectification process,

(29 July 2000, NOAA-14/band 2)

National borders and hydrographic (Dam, lake etc.) data were overlaid as vector data to all of the rectified images (Figure 5.8) to test the accuracy of the rectification process. This vector data were exactly overlaid to 25 of 32 rectified images (Figure 5.10). However, this vector data were not exactly overlaid to 7 of 32 rectified images (Figure 5.9). For this reason, these images were rectified again with their new GCP's.

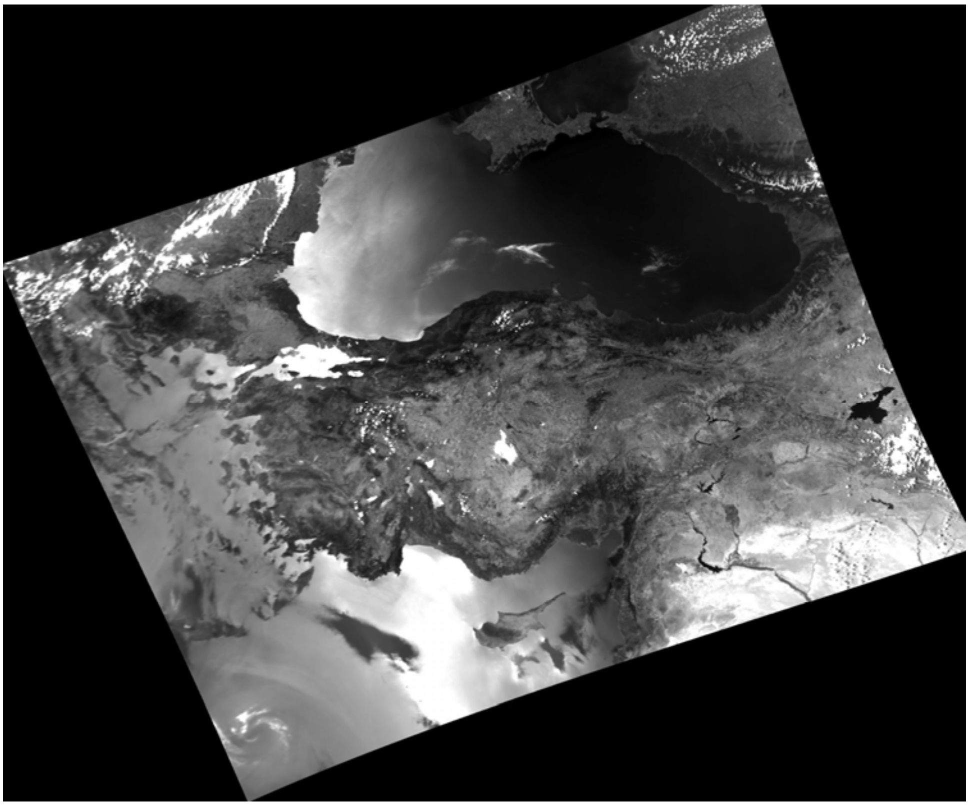

Figure 5.8 Rectified image (29 July 2000, NOAA-14/band 2)

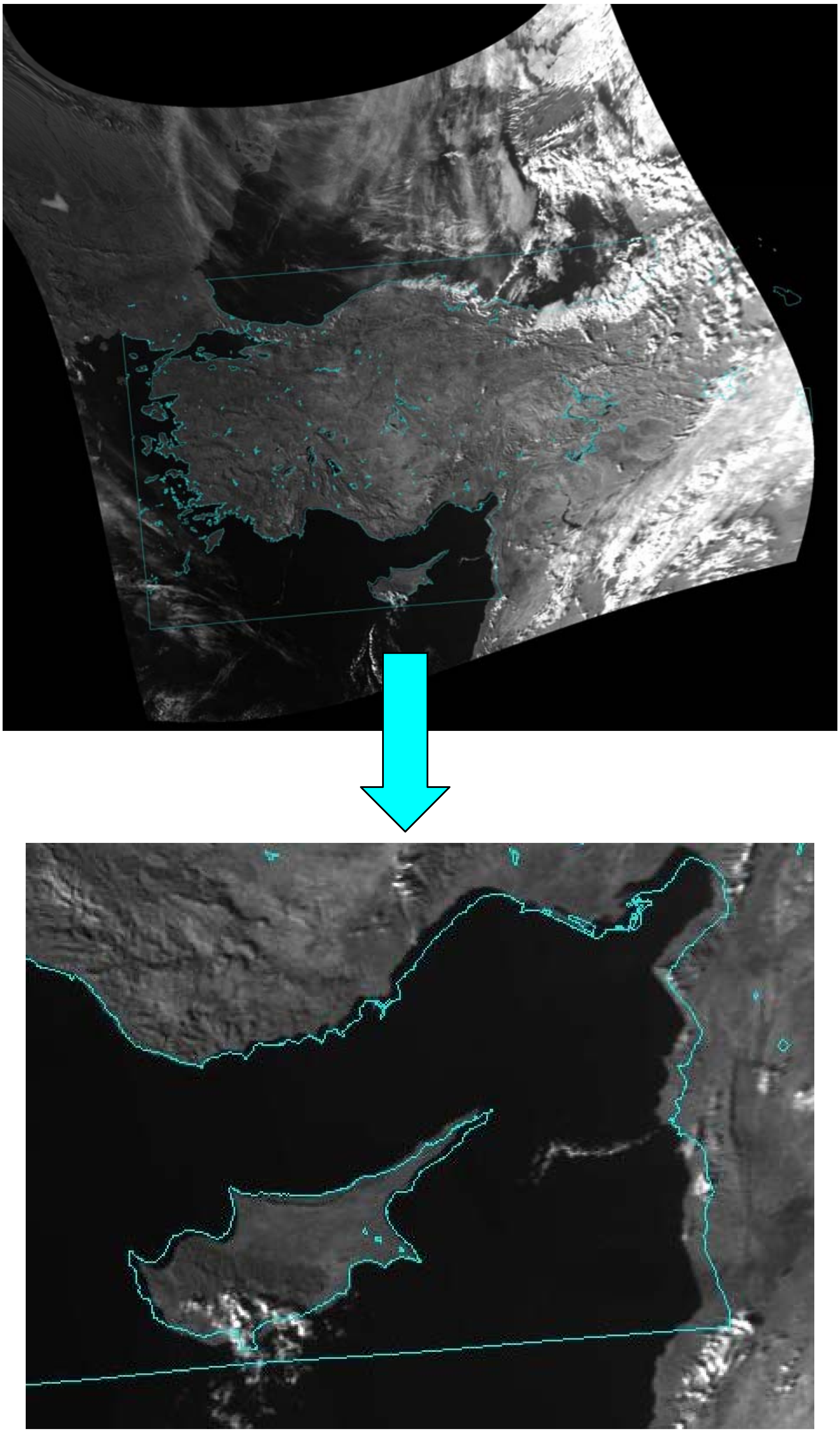

Figure 5.9 Rectified image (31 October 1999, NOAA-14/band2)

(with national borders & hydrographic data)

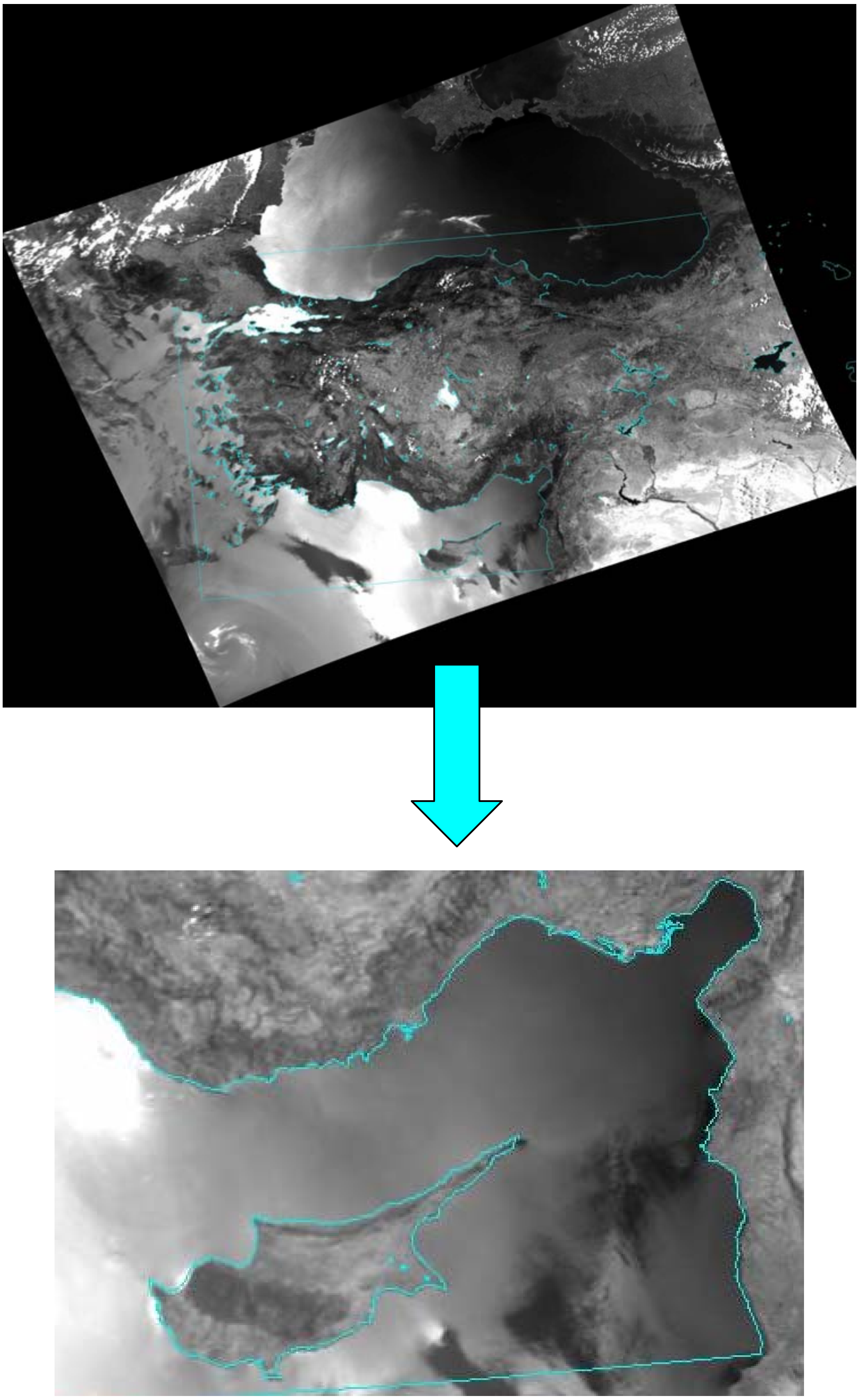

Figure 5.10 Rectified image (29 July 2000, NOAA-14/band2)
(with national borders & hydrographic data)

Table 5.3 Ground Control Point (GCP) numbers and RMS errors of used NOAA-AVHRR images

File name	Date	GCP	±RMS	Order of transformation
N14h1333.039	February 8,2001	11	0.74	2
ITU-CSCRS-2	February 8, 2004	10	0.58	2
N14h1318.062	March 2,2000	12	0.49	2
N14h1242.074	March 14,2000	11	0.61	2
N12h1405.069	March 10, 2001	15	0.65	2
ITU-CSCRS-1	March 1, 2004	12	0.49	2
N14h1318.097	April 6,2000	16	0.81	2
N14h1427.119	April 29,2001	11	0.25	2
N14h1115.130	May 10,1997	16	0.51	2
N14h1429.144	May 24,2001	12	0.41	2
N14h1446.151	May 31,2001	14	0.30	2
N14h1540.145	May 25,2002	14	0.55	2
N15h1627.139	May 19,2002	14	0.27	2
N14h1335.165	June 13,2000	14	0.53	2
N14h1403.163	June 12,2001	14	0.91	2
N14h1346.190	July 8,2000	18	0.53	2
N14h1303.211	July 29,2000	15	0.92	2
N14h1458.192	July 11,2001	19	0.62	2
N14h1508.188	July 7,2002	15	0.81	2
N14h1545.185	July 4,2002	15	0.62	2
N14h1258.220	August 7,2000	14	0.68	2
N14h1317.227	August 14,2000	16	0.84	2
N15h1601.239	August 15, 2001	11	0.77	2
N15h0531.224	August 12,2002	16	0.65	2
N14h1246	September 17,2001	10	0.69	2
N15h0527.250	September 7,2002	13	0.55	2
N15h1611.187	September 17,2002	19	0.67	2
N14h1314.304	October 31,1999	14	0.78	2
N14h1312.279	October 5,2000	11	0.84	2
N14h1240.307	November 3,1999	13	0.41	2
N14h1333.320	November15, 2000	12	0.66	2
N14h1242.351	December 17, 1999	10	0.31	2

All rectified 32 images were taken as one image data set by putting all into one single file and then overlaid in RGB display. 10 of 32 images were seen as distorted (having some offsets in x and y) in visual analyze (Figure 5.11). These distorted images were rectified again with their new GCP's. Then, all images were overlaid again with each others to test the accuracy of the rectification (Figure 5.12).

SPOT images were processed as Level 2A. In this correction, images were corrected by normalizing CCD response to compensate for radiometric variations due to detector sensivity. Geometric corrections were also done with Level 2A correction to match a standart map projection (UTM WGS 84), without using ground control points. At the end, location accuracy was obtained better than 350 metres for SPOT 2 and 4 (the mean elevation was taken constant in this process). [25]

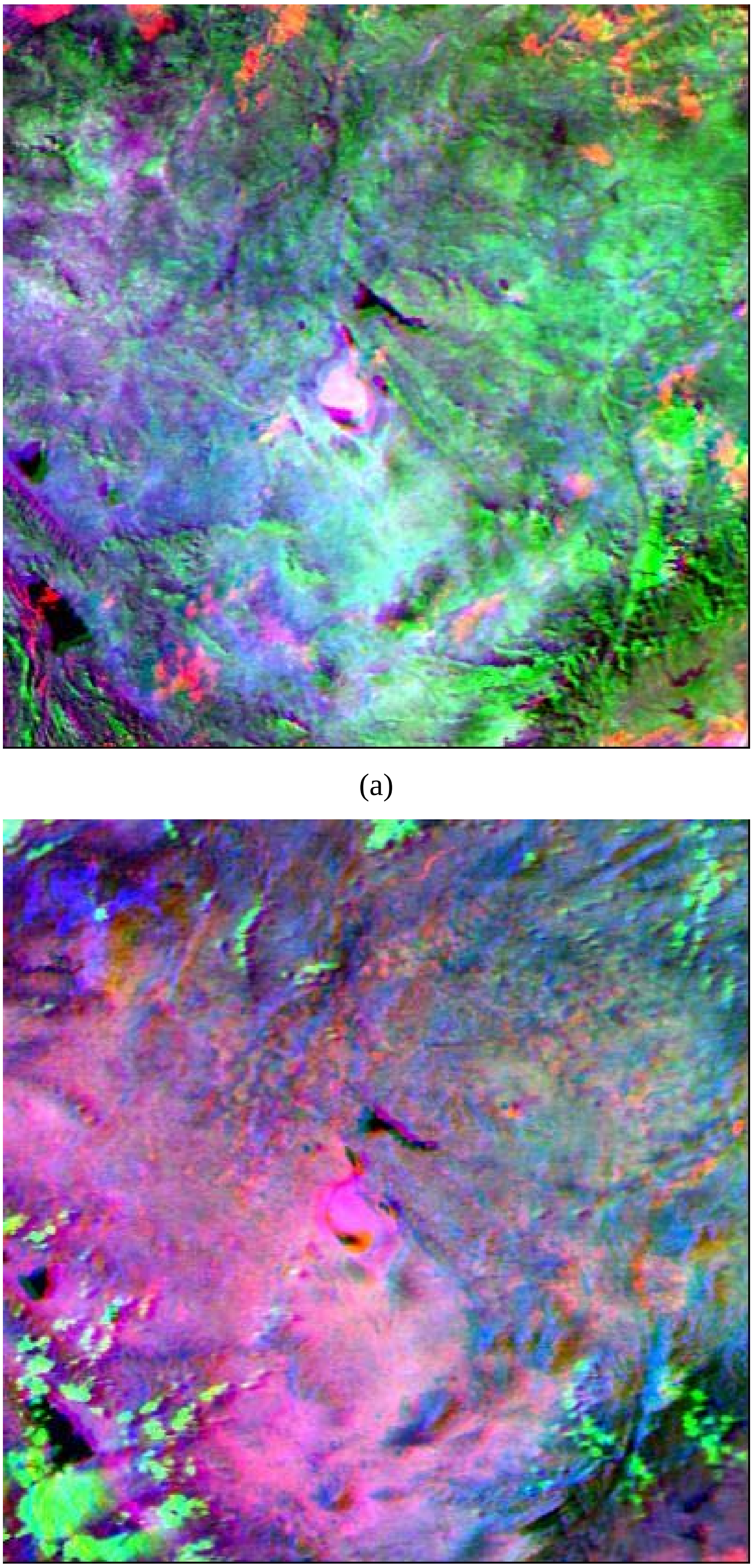

(a)

(b)

Figure 5.11 False color composite, distorted images

(a) RGB: 7 September 2002-31 October 1999-12 August 2002, NOAA-14/bant 2

(b) RGB: 12 August 2002-11 July 2001-17 September 2002, NOAA-14/bant 2

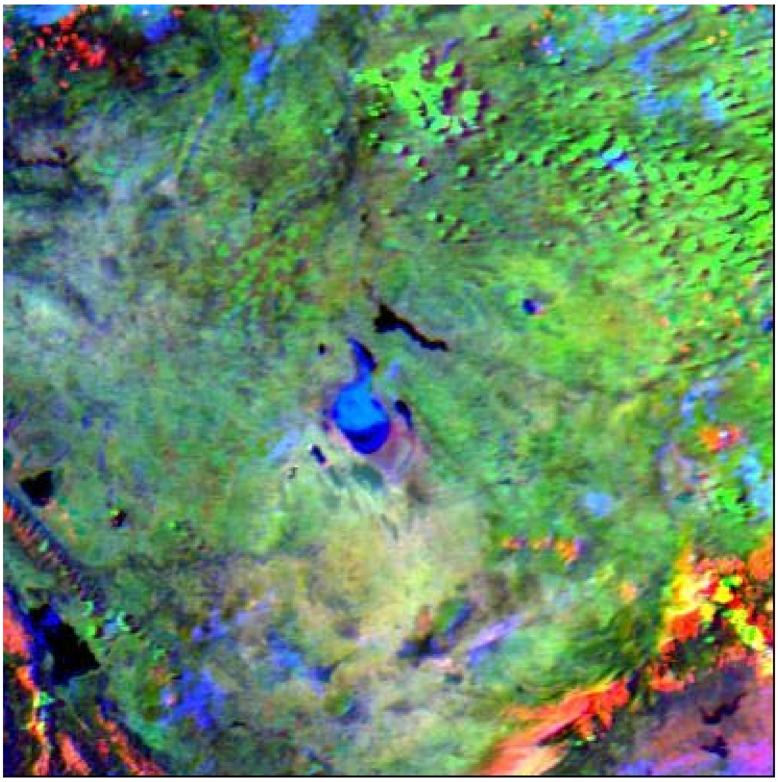

(a)

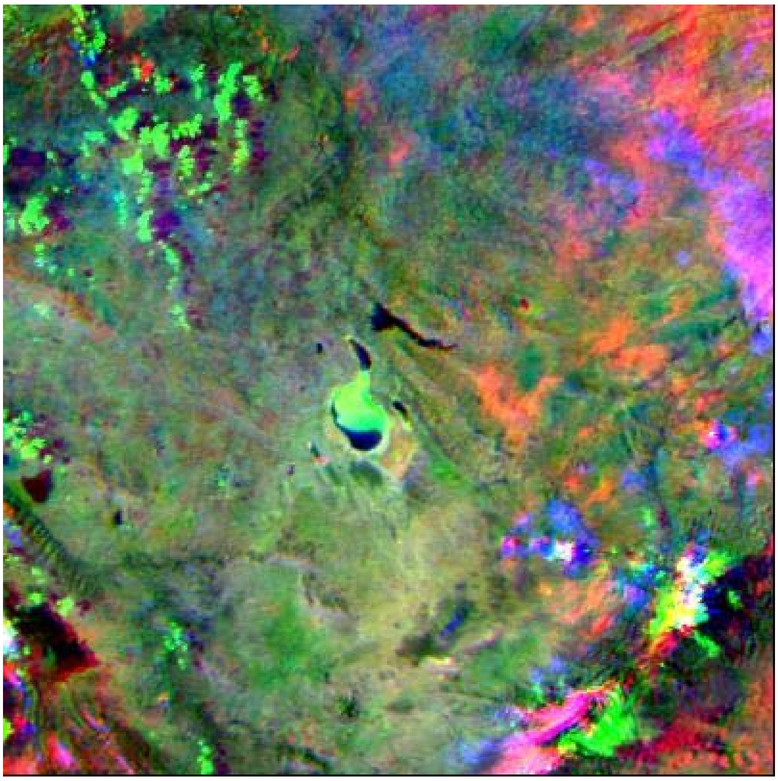

(b)

Figure 5.12 False color composite images

(a) RGB: 2 March 2000-31 May 2001-7 September 2002, NOAA-14/bant 2

(b) RGB: 10 March 2001-7 July 2002-17 December 1999, NOAA-14/bant 2

5.3.3 Image Enhancement

5.3.3.1 Contrast Enhancement

In this study, contrast enhancement methods were applied for all images for a better discrimination between water bodies and land cover. Since the discrimination of the linear features in segmentation method was better, linear contrast enhancement method was preferred for many NOAA-AVHRR images. Furthermore, Histogram equalization enhancement method was used for few NOAA-AVHRR images for a better discrimination (Figure 5.13).

SPOT XS/XI images were processed with linear contrast enhancement. Although, the Gaussian and Equalization enhancement methods were applied to them, linear contrast enhancement method was found more successful for discriminating water bodies and land cover (Figure 5.14).

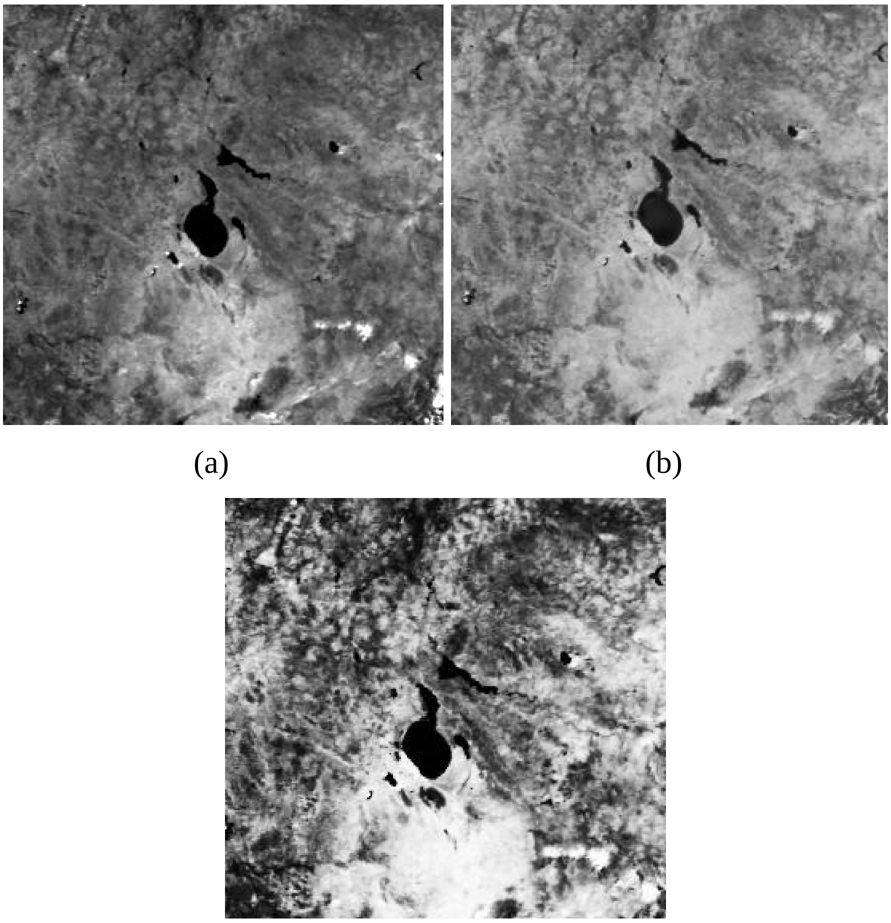

(a) (b)

(c)

Figure 5.13 Effects of contrast enhancement on 6 April 2000 image, (NOAA-14/band 2)
(a) Linear enhancement, (b) Gaussian enhancement, (c) Equalization enhancement

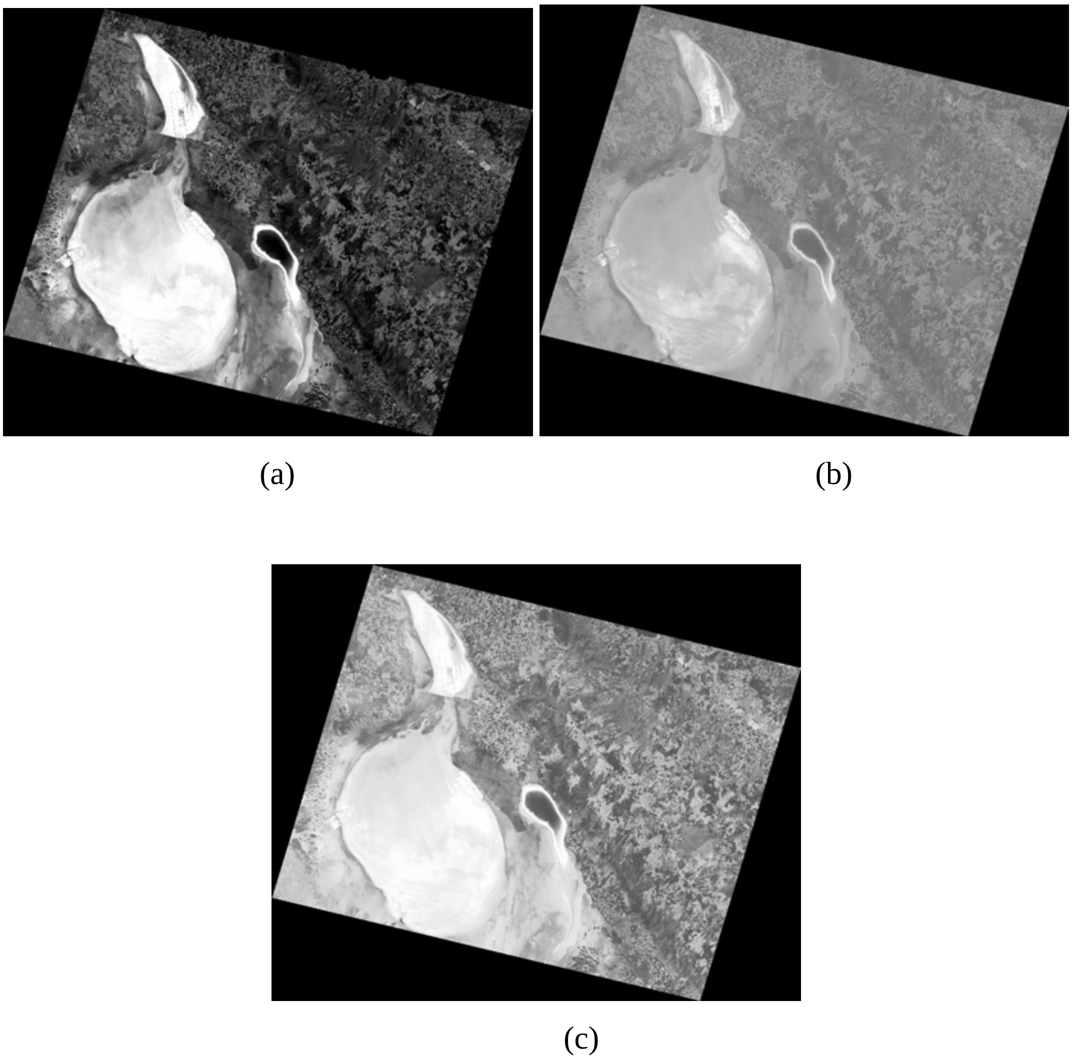

Figure 5.14 Effects of contrast enhancement on 18 August 2005 image (SPOT XS/band 3)
(a) Linear enhancement, (b) Gaussian enhancement, (c) Equalization enhancement

5.4 Water Body Area Calculation

Salt Lake region were cropped from all rectified NOAA-AVHRR images. Band 2 of all NOAA-AVHRR images and band 3 of SPOT XS/XI images were used to calculate water body areas on Salt Lake. Since these bands are near infrared channels, in this channel, discrimination between water body and land cover is apparent due to reflectance properties. Water body areal extent of Salt Lake was calculated with three different techniques. These techniques are segmentation, digitizing and unsupervised classification (ISODATA method). Water body areal extents of Salt Lake calculated with all these techniques, were given in Table 5.4.

5.4.1 Segmentation Method

Segmentation Method for NOAA-AVHRR images

Segmentation method was applied to band 2 of NOAA-AVHRR images. In this process, minimum and maximum thresh values were taken as 0 and 12 in most of the images. Minimum population was taken as 200 pixels to form a segment.

Discrimination between water body and land cover areas in wet season images were done easily. Because, deep water and land cover reflectance are very different from each other in near infrared region (Figure 5.15 (a)).

On the other hand, it was difficult to discriminate water body from land cover areas in dry season images. Water reflectance varies with its depth. Shallow water reflectance is higher than deep water reflectance. Lake shallowed over dry season. Since shallow water reflectance is slightly different from land cover areas reflectance, thus, discrimination between water body and land cover in dry season images was difficult with segmentation method (Figure 5.15 (b)).

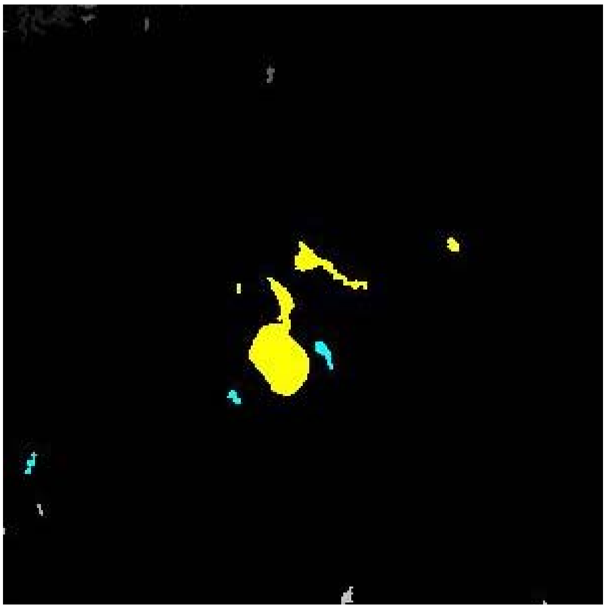

(a) 6 April 2000, NOAA-14/band 2

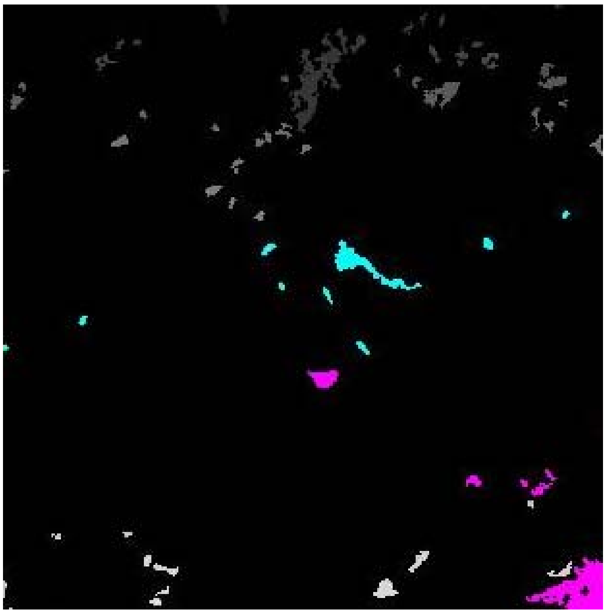

(b) 29 July 2000, NOAA-14/band 2

Figure 5.15 Segmentation method for NOAA-AVHRR images

Segmentation Method for SPOT XS/XI images

Segmentation method was applied to band 3 of SPOT XS/XI images. For SPOT XS image, minimum and maximum thresh values were taken as 60 and 130. Minimum population was taken as 100 pixels to form a segment (Figure 5.16 (a)). For SPOT XI image, minimum and maximum thresh values were taken as 8 and 35. Minimum population was taken as 200 pixels to form a segment (Figure 5.16 (b)). Like as NOAA-AVHRR images, it was difficult to discriminate water body and land cover areas in dry season image. On the contrary, discrimination was easy for wet season images.

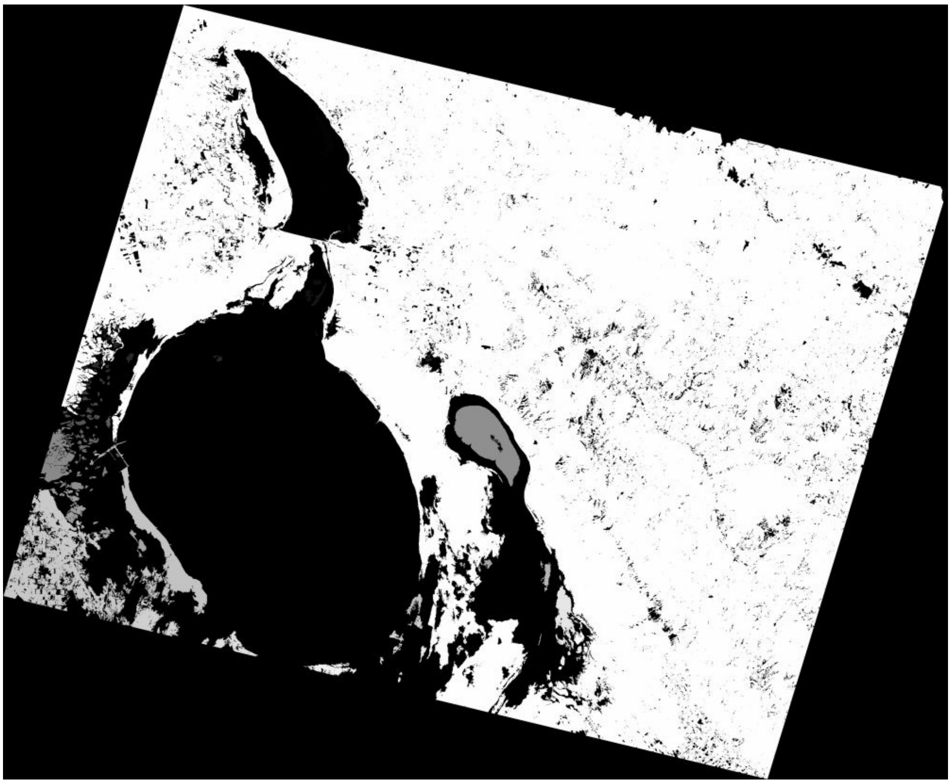

(a) 18 August 2005, SPOT XS/band 3

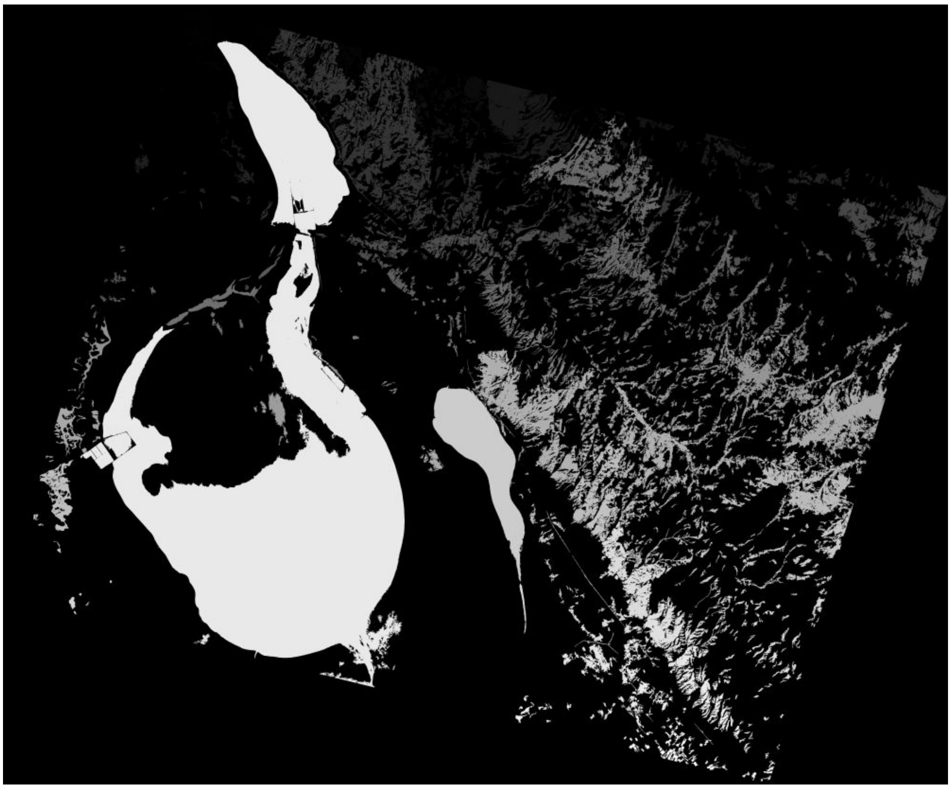

(b) 24 March 2005, SPOT XI/band 3

Figure 5.16 Segmentation method for SPOT XS/XI images

5.4.2 Digitizing Method

On-screen digitizing method was applied to all NOAA-AVHRR (Figure 5.17) and SPOT XS/XI (Figure 5.18) images. Since this method relying on visual interpretation, shallow water body could be added to whole water body areas. Thus, water body areal extents calculated with this method are greater than other methods.

Digitizing Method for NOAA-AVHRR images

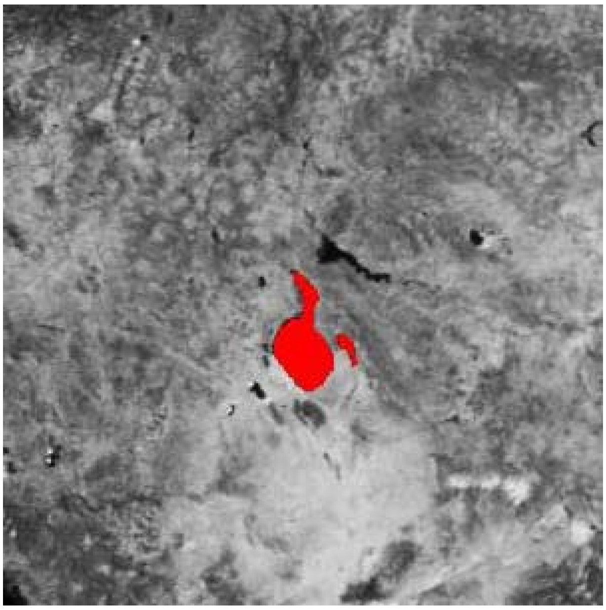

(a) 6 April 2000, NOAA-14/band 2

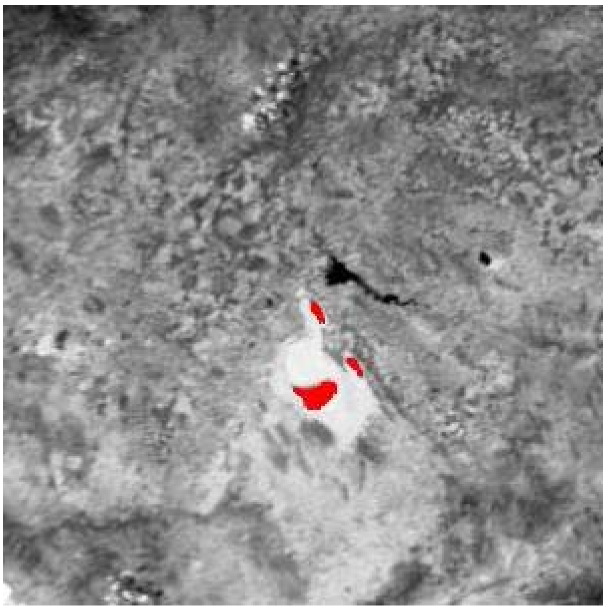

(b) 29 July 2000, NOAA-14/band 2

Figure 5.17 Digitizing method for NOAA-AVHRR images

Digitizing Method for SPOT XS/XI images

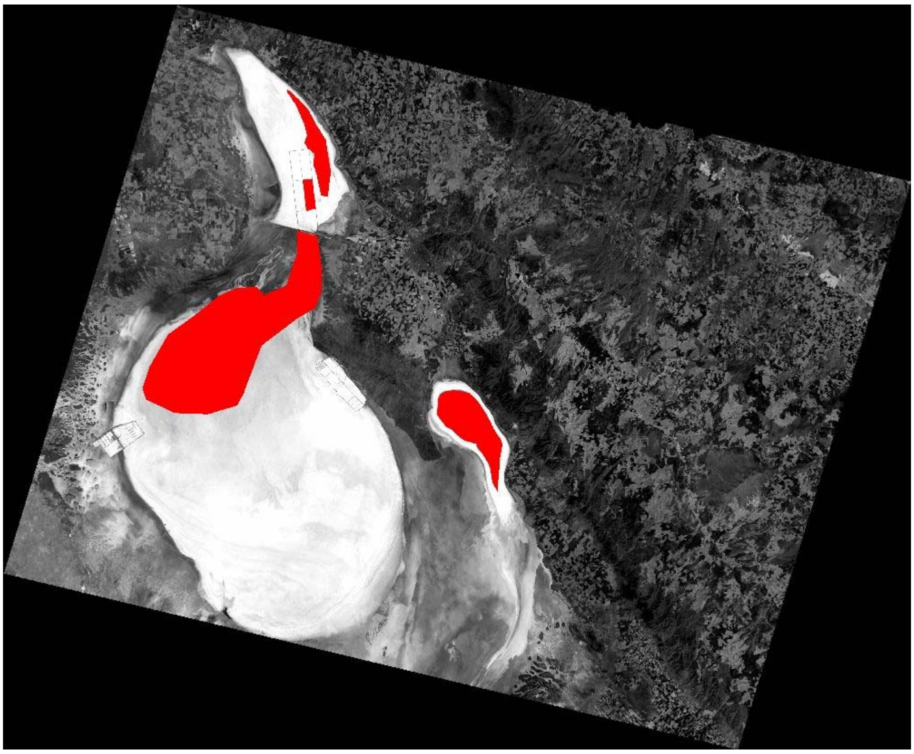

(a) 18 August 2005, SPOT 2/XS, band 3

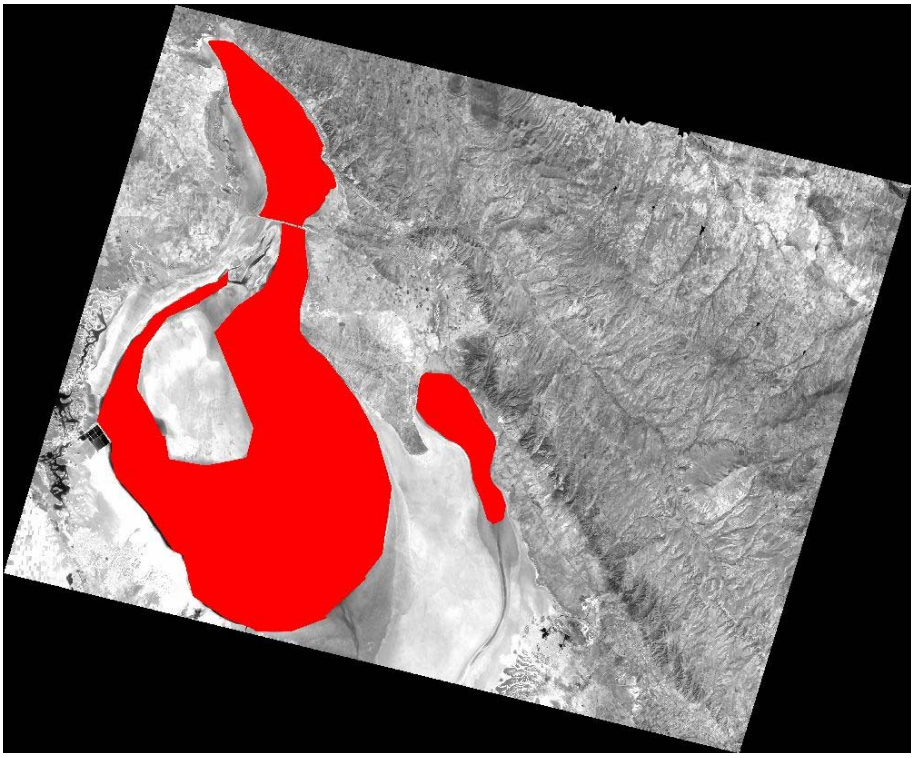

(b) 24 March 2005, SPOT 4/XI, band 3

Figure 5.18 Digitizing method for SPOT XS/XI images

5.4.3 ISODATA Classification Method

ISODATA Classification Method for NOAA-AVHRR images

While classifying NOAA-AVHRR images with ISODATA Classification method, 5 classes were created and 3 iterations done. Minimum 100 pixels exist in one class regarding to selected parameter. Since the discrimination between water body and land cover areas is easier, infrared channels (either only channel 2 or both channel 2 and 3) of NOAA-AVHRR images were used.

Discrimination between water body and land cover areas in wet season images were done easily with this method like as segmentation method (Figure 5.19 (a)).

On the contrary, there was a difficulty again in discrimination between water body and land cover areas in dry season images with this method (Figure 5.19 (b)).

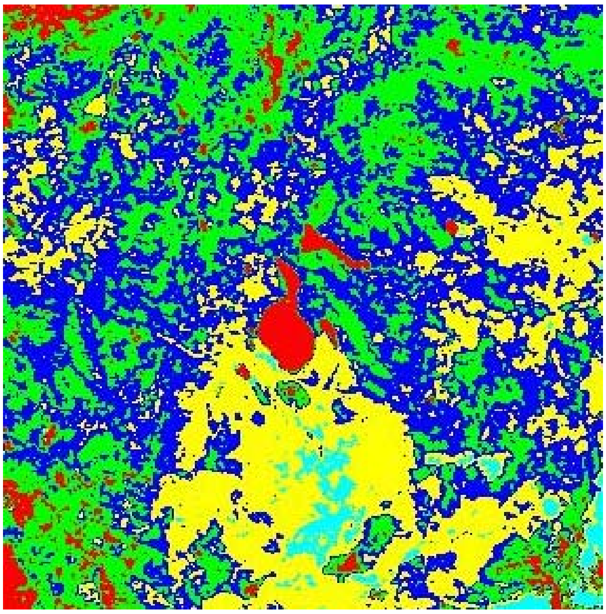

(a) 6 April 2000, NOAA-14/band 2

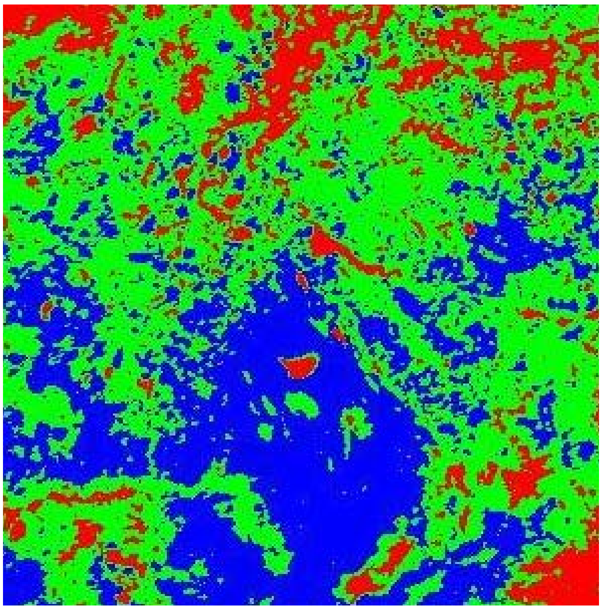

(b) 29 July 2000, NOAA-14/band 2

Figure 5.19 ISODATA Classification method for NOAA-AVHRR images

ISODATA Classification Method for SPOT XS/XI images

ISODATA Classification method was also applied to SPOT XS/XI images. In these images, shallow and deep water areas can be seen visually. But, it is difficult to discriminate water body from land cover area with this method. Classes were mixing up with each other. 15 classes were created and 3 iteration used. After that, some classes combined with each other to calculate whole water body areal extent in images.

Discrimination between water body and land cover areas were done easily with this method for wet season images (Figure 5.20 (a)).

There was a difficulty again with dry season image (Figure 5.20 (b)). Areal extent calculated with this method is smaller than other two methods for dry season image.

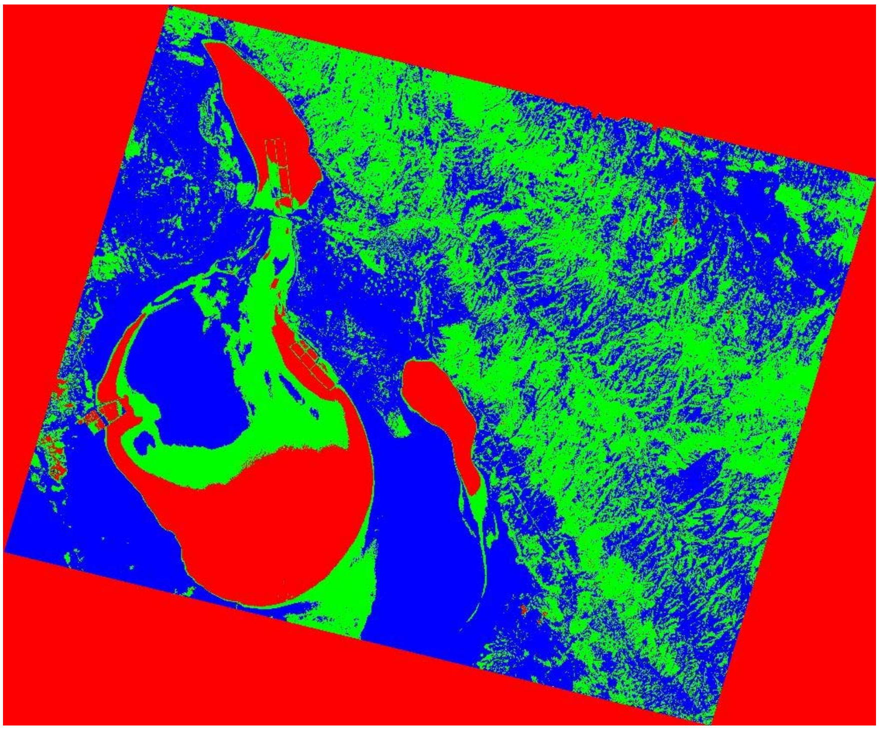

(a) 24 March 2005, SPOT 4/XI, band 3

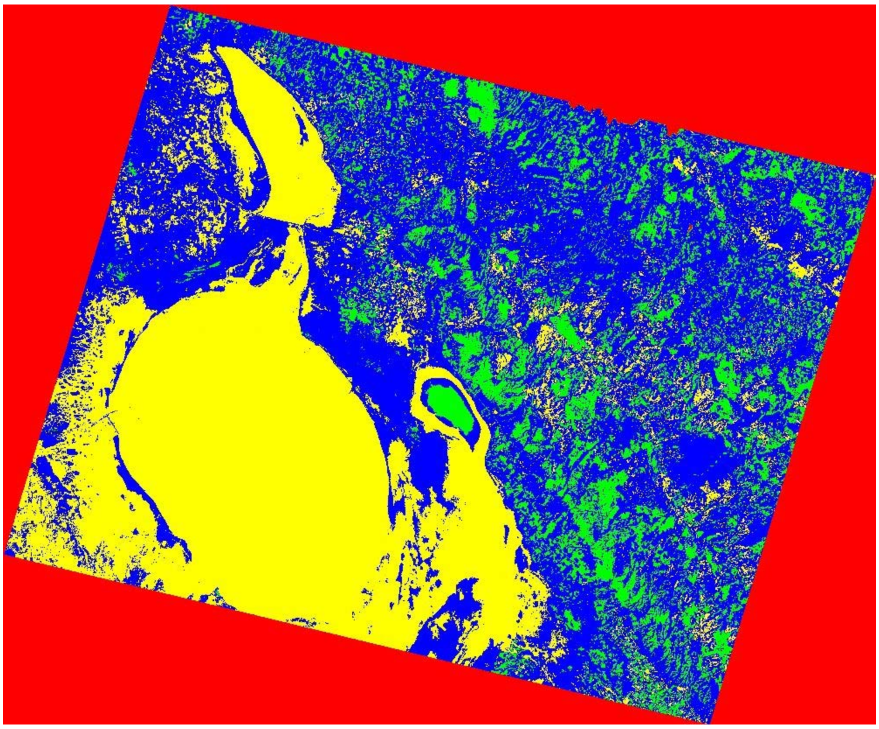

(b) 18 August 2005, SPOT 2/XS, band 3

Figure 5.20 ISODATA Classification method for SPOT XS/XI images

Table 5.4 Areal extent results in Salt Lake

Image ID	Date of image taken	Area of segmentation (hectares)	Area of digitizing (hectares)	Area of isodata class. (hectares)	Precipitation (mm)
n14h1333.039	February 8, 2001	12,100.000	15,400.000	14,700.000	11.68
ITU-CSCRS-2	February 8, 2004	85,500.000	89,600.000	89,200.000	9.65
n14h1318.062	March 2, 2000	88,200.000	97,000.000	96,400.000	12.2
n14h1242.074	March 14, 2000	76,000.000	77,200.000	76,600.000	12.2
n12h1405.069	March 10, 2001	38,000.000	39,000.000	35,200.000	5.58
ITU-CSCRS-1	March 1, 2004	87,000.000	89,700.000	92,500.000	2.29
Spot-4	March 24, 2005	85,187.755	77,861.000	69,188.200	10.67
n14h1318.097	April 6, 2000	93,100.000	95,200.000	96,600.000	40.12
n14h1427.119	April 29, 2001	19,200.000	21,400.000	21,300.000	24.38
n14h1115.130	May 10, 1997	85,100.000	93,600.000	96,100.000	41.91
n14h1429.144	May 24, 2001	40,700.000	43,100.000	47,700.000	65.28
n14h1446.151	May 31, 2001	42,200.000	41,600.000	42,700.000	65.28
n14h1540.145	May 25, 2002	71,200.000	99,500.000	100,100.000	25.14
n15h1627.139	May 19, 2002	87,500.000	94,000.000	78,700.000	25.14
n14h1335.165	June 13, 2000	75,700.000	79,900.000	82,100.000	16.01
n14h1403.163	June 12, 2001	16,500.000	16,600.000	12,700.000	0.76
n14h1346.190	July 8, 2000	43,200.000	47,600.000	49,600.000	0
n14h1303.211	July 29, 2000	25,000.000	23,700.000	17,200.000	0
n14h1458.192	July 11, 2001	7,600.000	10,400.000	12,000.000	2.55
n14h1508.188	July 7, 2002	26,500.000	29,100.000	22,500.000	5.59
n14h1545.185	July 4, 2002	26,400.000	35,200.000	38,900.000	5.59
n14h1258.220	August 7, 2000	13,800.000	14,900.000	8,400.000	4.32
n14h1317.227	August 14, 2000	10,400.000	14,500.000	12,100.000	4.32
n15h1601.239	August 15, 2001	8,400.000	8,600.000	5,500.000	4.06
n15h0531.224	August 12, 2002	16,800.000	12,400.000	7,900.000	8.64
Spot-2	August 18, 2005	10,310.000	18,907.000	2,365.000	0
n14h1246	September 17, 2001	11,000.000	7,800.000	2,900.000	6.09
n15h0527.250	September 7, 2002	9,300.000	9,100.000	4,300.000	66.55
n15h1611.187	September 17, 2002	26,900.000	31,600.000	25,900.000	66.55
n14h1314.304	October 31, 1999	11,000.000	15,700.000	17,300.000	19.3
n14h1312.279	October 5, 2000	10,900.000	9,900.000	10,400.000	32.52
n14h1240.307	November 3, 1999	12,200.000	16,000.000	9,000.000	0.25
n14h1333.320	November 15, 2000	17,000.000	18,100.000	12,600.000	27.18
n14h1242.351	December 17, 1999	8,000.000	16,500.000	10,600.000	5.33

Water body areal extents calculated with segmentation, digitizing and ISODATA Classification techniques were slightly different from each other. Generally, water body areal extents calculated with digitizing technique greater than segmentation and ISODATA Classification techniques. It was thought that visual interpretation was more effective and easy, therefore this difference in the results were reasonable.

It was also seen that areal extents are being changed regarding to temproral and annual base (Figure 5.20). Meteorological data of Konya were used for interpreting the results obtained (Figure 5.21). Thus, meteorological data and areal extent results were seen compatible.

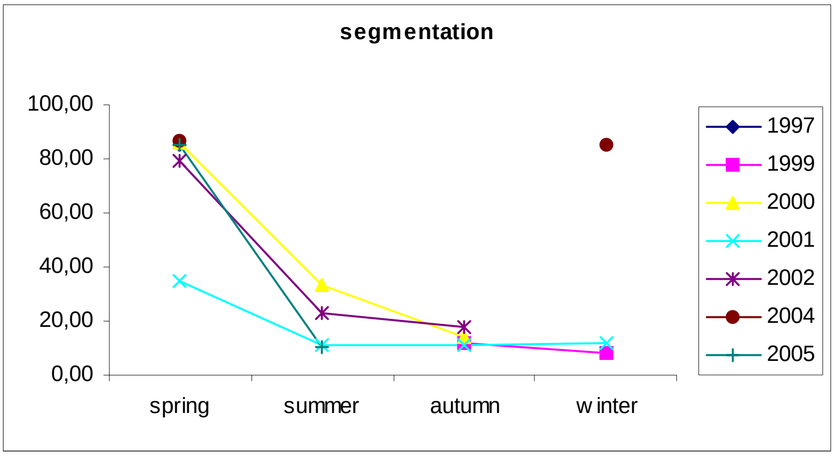

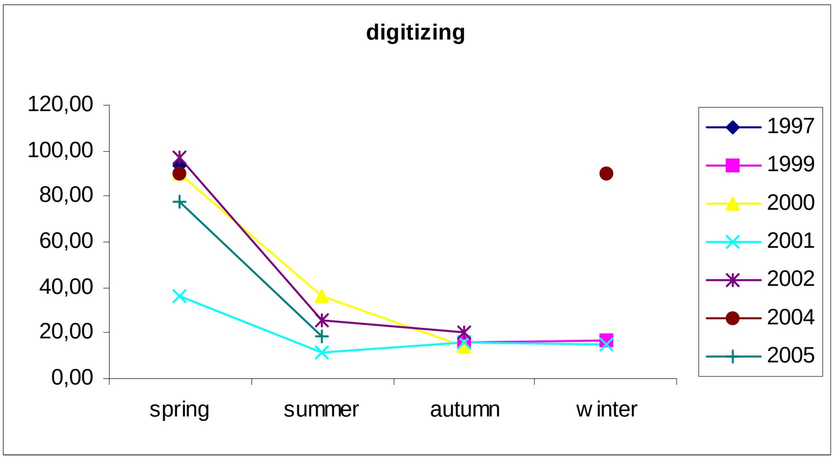

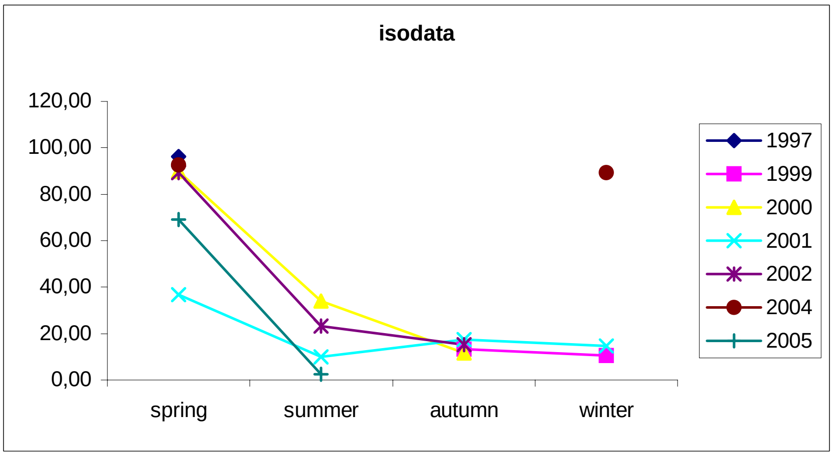

Figure 5.21 Areal extents calculated by 3 methods

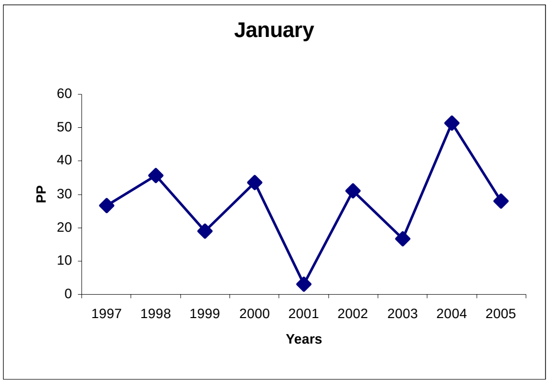

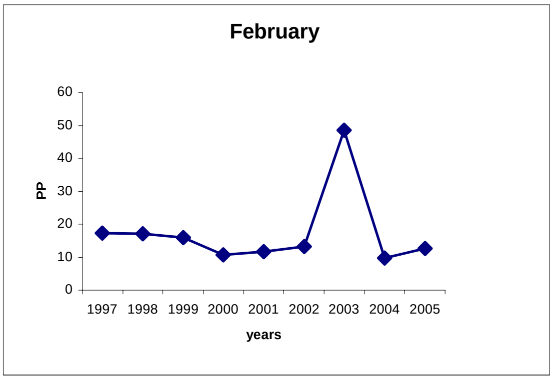

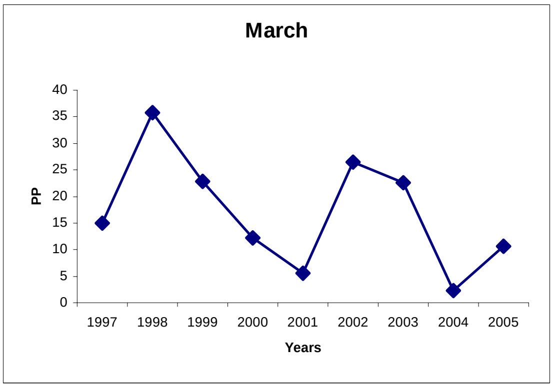

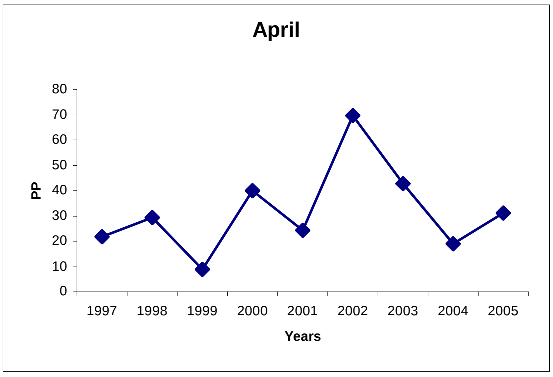

Figure 5.22 Monthly Total Precipitation for the period (1997-2005)

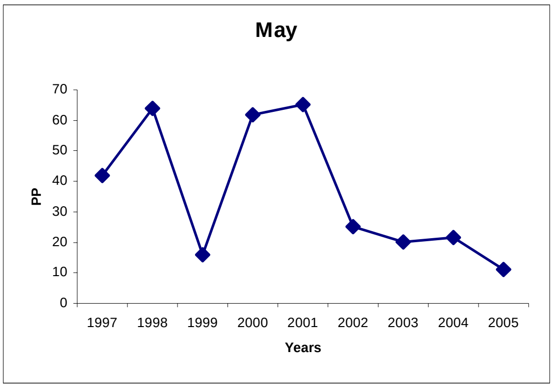

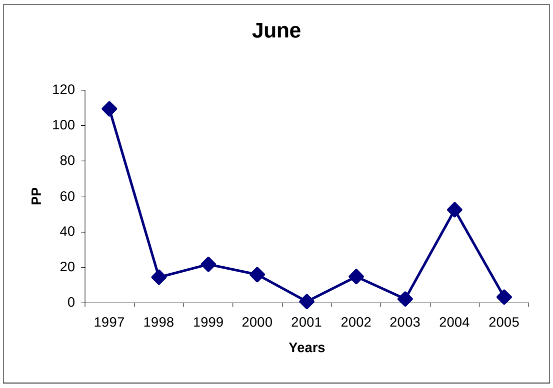

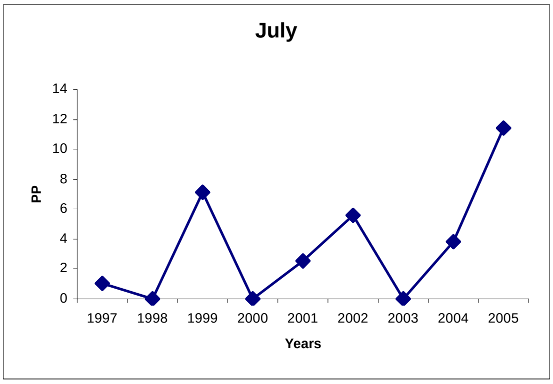

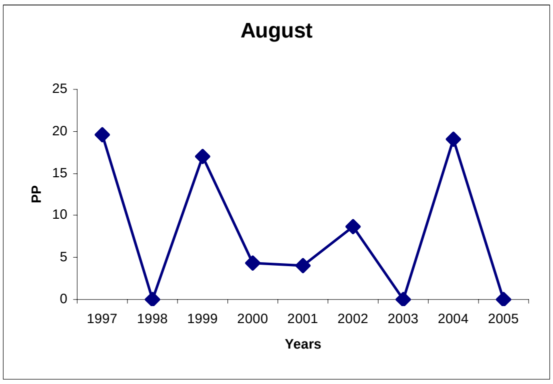

Figure 5.22 (Cont.)

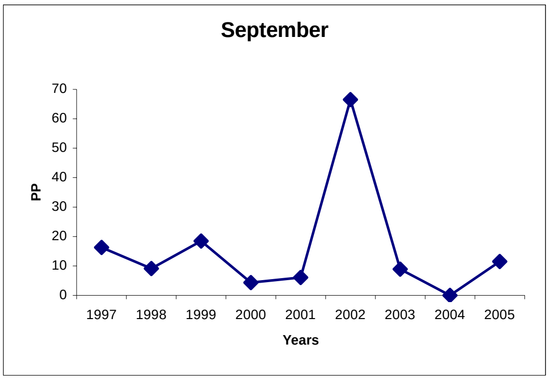

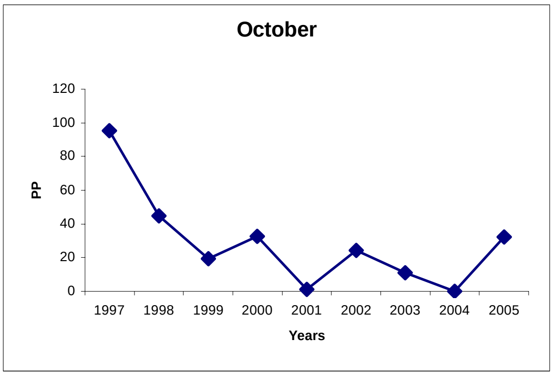

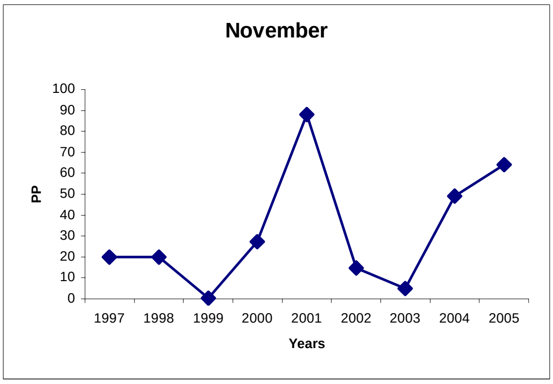

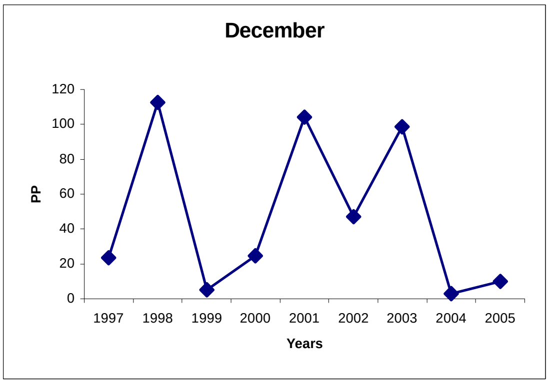

Figure 5.22 (Cont.)

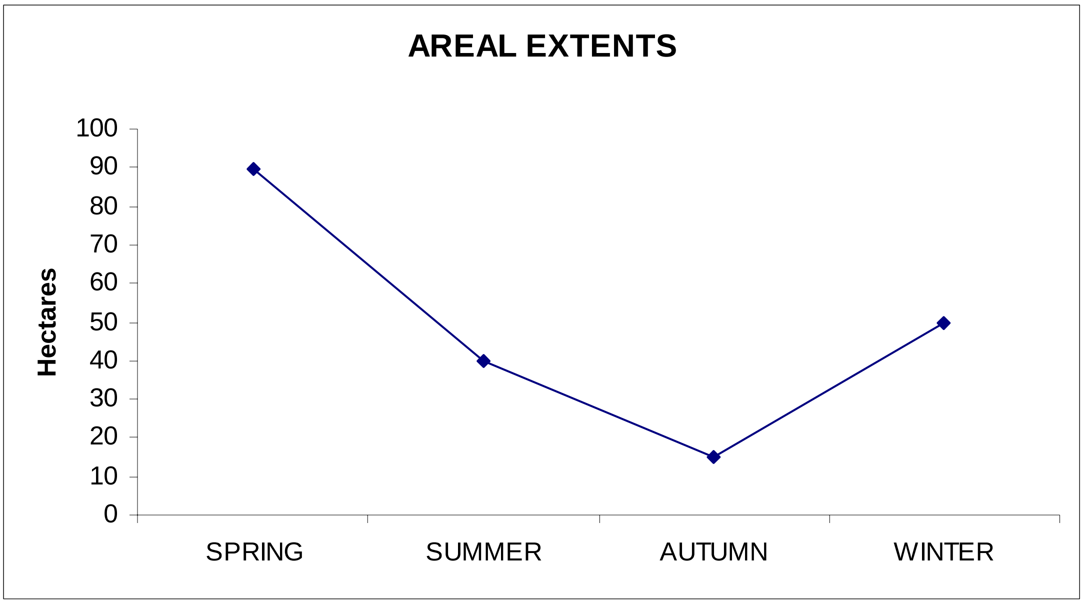

Figure 5.23 Average areal extent results

Water body areal extents calculated with segmentation, on-screen digitizing and ISODATA classification techniques were slightly different from each other. Average values of these results were calculated for each season except the values of year of 2001 (Figure 5.23). The results showed that the water body areal extent was 89.6 ha for spring, 39.8 ha for summer, 14.9 ha for autumn and 49.9 ha for winter. Results of year of 2001 weren’t used in the average calculation since the values were too low due to drought observed in this year. Meteorological data of Konya were also confirmed this outcome with very low precipitation values. Average precipitation amount except the values of year of 2001 for each season were also seen compatible with the analysis results.

6. CONCLUSION AND DISCUSSIONS

Salt lake being the second largest lake in Turkey is a very important source of salt for Turkey. It is also an important area for aquatic birds to spend their winter time, since covering very large area in winter and not freezing even coldest days. Aquatic birds habitat and also the ecosystem of the lake will be affected from the changes in areal extent of Salt Lake. Today, monitoring changes of water resources with remote sensing technique is an efficient and cost effective method. For this purpose, NOAA-AVHRR and SPOT XS/XI images (dated between 1997-2005) were used and processed to monitor the changes in Salt Lake.

In the analysis, three different techniques; segmentation, on-screen digitizing and unsupervised classification (ISODATA method), were used to calculate water body areal extent of Salt Lake.

In the segmentation method applied to band 2 of NOAA-AVHRR images and band 3 of SPOT XS/XI images, discrimination between water body and land cover areas in wet season images were done easily, since deep water and land cover reflectance are very different from each other in near infrared region. However, water reflectance varies with its depth, therefore shallow water reflectance is generally higher than deep water reflectance as seen in the Lake over dry season. Since shallow water reflectance is slightly different from land cover areas reflectance, discrimination between water body and land cover in dry season images was difficult with segmentation method.

In the on-screen digitizing method applied to all NOAA-AVHRR and SPOT XS/XI images, shallow water body was also added to whole water body areas since this method is relying on visual interpretation. Thus, water body areal extents calculated with this method are greater than other methods.

In the ISODATA classification method applied to all NOAA-AVHRR and SPOT-XS/XI images, 2nd (or 2nd and 3rd) channel(s) of NOAA-AVHRR images and 3rd channel of SPOT XS/XI images were used as spectral subset since the discrimination between water body and land cover areas is more distinct in near infrared channels. Discrimination between water body and land cover areas in wet season images were done easily with this method like as segmentation method. On the contrary, there was a difficulty again in discrimination between water body and land cover areas in dry season images. In SPOT XS/XI images, shallow and deep water areas can be seen visually. But, it was difficult to discriminate water body from land cover area with this method. Classes were mixed up with each other. 15 classes were created and 3 iteration used. After that, some classes combined with each other to calculate whole water body areal extent. Discrimination between water body and land cover areas were done easily with this method for wet season images. There was a difficulty again with dry season image. Areal extent calculated with this method is smaller than other two methods for dry season image

Water body areal extents calculated with segmentation, on-screen digitizing and ISODATA classification techniques were slightly different from each other. Average values of these results were calculated for each season except the values of year of 2001. The results showed that the water body areal extent was 89.6 ha for spring, 39.8 ha for summer, 14.9 ha for autumn and 49.9 ha for winter. Results of year of 2001 weren't used in the average calculation since the values were too low due to drought observed in this year. Meteorological data of Konya were also confirmed this outcome with very low precipitation values. Average precipitation amount except the values of year of 2001 for each season were also seen compatible with the analysis results.

As can be seen from this study, remote sensing methods are effective tool for regional water resources monitoring. Although the data set used was not enough statisticaly to conclude seasonal tendency in the area, however it was shown that low or medium resolution satellite data can be used for this type analysis successfully.

REFERENCES

[1] Lillesand T.M, and Kiefer R.W,1987. Remote sensing and image interpretation, John Willey & Sons

[2] URL: http://www.ccrs.nrcan.gc.ca

[3] URL: http://www.gisdevelopment.net/tutorials/tuman008.htm

[4] URL: http://rst.gsfc.nasa.gov

[5] Lintz, J.Jr-Simonett, D.S.(Ed), 1976. Remote sensing of environment, Addison & Wesley Publishing Company

[6] URL: http://www.uwm.edu/Course/416-403/emrad4.pdf

[7] Rees, W.G., 1990. Topics in remote sensing 1, Physical principles of remote sensing, Cambridge University Press

[8] URL: http://www.wamis.org/agm/pubs/agm8/Paper-2.pdf

[9] URL: http://earthobservatory.nasa.gov/Library/RemoteSensing/remote_04.html

[10] URL: http://gs.mdacorporation.com/

[11] URL: http://www.ga.gov.au/acres/prod_ser/noaadata.htm

[12] URL: http://www.ga.gov.au/acres/prod_ser/modisdata.htm

[13] URL: http://www.ga.gov.au/acres/prod_ser/landdata.jsp

[14] URL: http://www.spotimage.fr/html/_167_224_555_233_.php

[15] URL: http://www.wwf.org.tr

[16] URL: http://gaia.amnh.org/remote_sensing/guides/image_interp.html

[17] URL: http://www.icimod-gis.net

[18] URL: http://www.ucalgary.ca/UofC/faculties/SS/GEOG/Virtual/

[19] URL: http://www.csr.utexas.edu/rs/sensors/optical.html

[20] URL: http://micro.magnet.fsu.edu/primer/java/reflection/specular/

[21] URL: http://www.geo.mtu.edu/rs/

[22] URL: http://telsat.belspo.be/BEo/en/satellites/spot.htm

[23] URL: http://history.nasa.gov/SP-4012/vol6/vol_vi_ch_1.pdf

[24] ERDAS Field Guide

[25] URL: http://www.cscrs.itu.edu.tr

[26] URL: http://www.yeniller.de

[27] URL: www.uni-kiel.de/castle/ch3/s3l7p040.htm

[28] URL: http://ceos.cnes.fr:8100/cdrom-00b2/ceos1/irsd/page/dre4.htm

[29] URL: http://rangeview.arizona.edu/Glossary/spares.html

[30] URL: http://www.spaceimaging.com

[31] URL: http://www.profc.udec.cl/~gabriel/tutoriales/rsnote

[32] URL: http://www.cevre.org

[33] URL: http://www.worldbank.org

[34] URL: http://www.amesremote.com/section1.htm

[35] URL: http://www.cnr.berkeley.edu/~gong/textbook/chapter5/html/home5.htm

[36] URL: http://www.cas.sc.edu/geog/rslab/Rscc/mod6/6-3/nonlinear.html

BIOGRAPHY

Yelda Türkan was born in Balıkesir in 1981. She was graduated from Çanakkale Science High School in June 1998. She has completed double major degree in Istanbul Technical University. Her first BSc degree is from Geodesy and Photogrammetry Engineering, and she was ranked as 3rd in June 2003. Her second BSc degree is from Civil Engineering, from which she was graduated in January 2005. In September 2003, she has joined to the MSc programme of Satellite Communication and Remote Sensing at the same university. Besides her academic experiences, she has been working as project engineer in Bosphorus Technical Consulting Corporation since June 2005.